

## 1 **Activation of MAIT cells plays a critical role in viral vector vaccine immunogenicity**

2

3 Nicholas M. Provine<sup>1,\*</sup>, Ali Amini<sup>1</sup>, Lucy C. Garner<sup>1</sup>, Christina Dold<sup>2</sup>, Claire Hutchings<sup>3</sup>, Michael  
4 E.B. FitzPatrick<sup>1</sup>, Laura Silva Reyes<sup>2</sup>, Senthil Chinnakannan<sup>3</sup>, Blanche Oguti<sup>2</sup>, Meriel Raymond<sup>2</sup>,  
5 Stefania Capone<sup>4</sup>, Antonella Folgori<sup>4,5</sup>, Christine S. Rollier<sup>2</sup>, Eleanor Barnes<sup>3</sup>, Andrew J.  
6 Pollard<sup>2</sup>, Paul Klenerman<sup>1,3,\*</sup>

7

8 <sup>1</sup> Translational Gastroenterology Unit, Nuffield Department of Medicine, University of Oxford

9 <sup>2</sup> Oxford Vaccine Group, Department of Paediatrics, University of Oxford, and the NIHR Oxford  
10 Biomedical Research Centre

11 <sup>3</sup> Peter Medawar Building for Pathogen Research, University of Oxford

12 <sup>4</sup> Reithera, SRL

13 <sup>5</sup> Nouscom, SRL

14 \* Corresponding authors: [nicholas.provine@ndm.ox.ac.uk](mailto:nicholas.provine@ndm.ox.ac.uk); [paul.klenerman@ndm.ox.ac.uk](mailto:paul.klenerman@ndm.ox.ac.uk)

15

16 **One sentence summary:** Robust immunogenicity of candidate adenovirus vaccine vectors  
17 requires the activation of unconventional T cells.

18

### 19 **Abstract**

20 Mucosal-associated invariant T (MAIT) cells can be activated by viruses through a cytokine-  
21 dependent mechanism, and thereby protect from lethal infection. Given this, we reasoned  
22 MAIT cells may have a critical role in the immunogenicity of replication-incompetent  
23 adenovirus vectors, which are novel and highly potent vaccine platforms. *In vitro*, ChAdOx1  
24 (Chimpanzee Adenovirus Ox1) induced potent activation of MAIT cells. Activation required  
25 transduction of monocytes and plasmacytoid dendritic cells to produce IL-18 and IFN- $\alpha$ ,  
26 respectively. IFN- $\alpha$ -induced monocyte-derived TNF- $\alpha$  was identified as a novel intermediate  
27 in this activation pathway, and activation required combinatorial signaling of all three  
28 cytokines. Furthermore, ChAdOx1-induced *in vivo* MAIT cell activation in both mice and  
29 human volunteers. Strikingly, MAIT cell activation was necessary *in vivo* for development of  
30 ChAdOx1-induced HCV-specific CD8 T cell responses. These findings define a novel role for  
31 MAIT cells in the immunogenicity of viral vector vaccines, with potential implications for  
32 future design.

33

34 **Body**

35 Mucosal-associated invariant T (MAIT) cells, an abundant T cell population in humans, bridge  
36 innate and adaptive immunity due to their ability to execute effector functions following  
37 cytokine stimulation in the absence of TCR signals(1). *In vivo*, MAIT cells can respond to  
38 viruses in this TCR-independent manner, and mediate protection against lethal infection via  
39 early amplification of local effector mechanisms(2-4). We reasoned that such focused activity  
40 could play a critical role in viral vaccine immunogenicity. Replication-incompetent adenovirus  
41 (Ad) vectors are novel and highly potent vaccine platforms for many human diseases(5). We  
42 therefore sought to determine if such vectors activate MAIT cells and if this activation impacts  
43 on vaccine immunogenicity.

44 Firstly, to determine if MAIT cells respond to Ad vectors, we stimulated human PBMCs  
45 for 24 h with increasing MOIs of Ad5 and ChAdOx1, two clinically-relevant vectors(6, 7).  
46 ChAdOx1 induced robust dose-dependent upregulation of IFN- $\gamma$ , CD69, and granzyme B by  
47 MAIT cells (Fig. 1A-C; Fig. S1A-D). In contrast, Ad5 only weakly activated MAIT cells even at  
48 the maximum dose (Fig. 1A-C). Activation in response to Ad vectors was confirmed using the  
49 MR1/5-OP-RU tetramer to identify MAIT cells (Fig. S1E). V $\delta$ 2+ T cells share many  
50 characteristics with MAIT cells(8, 9), and showed analogous Ad vector-induced activation  
51 (Fig. S1A, S1F).

52 We tested a wider range of Ad vectors including three species C-derived vectors (weak  
53 innate inducers(10-12)): Ad5(13), Ad6(13), and ChAdN13 (unpublished), and five non-  
54 species C vectors (strong innate inducers(10-12)): Ad35 (B)(13), Ad24 (D)(13), ChAdOx1  
55 (E)(13, 14), ChAd63 (E)(13), and ChAd68 (AdC68; E)(15). In response to stimulation with the  
56 various vectors there was a gradient of IFN- $\gamma$ , CD69, and granzyme B production by MAIT and  
57 V $\delta$ 2+ T cells, which resulted in greater average activation by non-species C as compared to C  
58 vectors (Fig. 1D-F; Fig. S1G-I), consistent with the above reports of differential innate immune  
59 activation by these families of vectors.

60 We next determined if MAIT and V $\delta$ 2+ T cells are activated following administration  
61 of Ad vectors to humans. We analyzed the activation of MAIT and V $\delta$ 2+ T cells and plasma  
62 cytokine levels on day -1 and day 1 following immunization of humans with  $5 \times 10^{10}$  vp of a  
63 novel ChAdOx1-MenB.1 vaccine (Fig. S2A, S2B). We observed modest, but statistically-

64 significant upregulation of CD69 on MAIT and V $\delta$ 2<sup>+</sup> T cells one day following ChAdOx1  
65 immunization (Fig. 1G, 1H), with no changes in cell frequency (Fig. S2C). The degree of MAIT  
66 and V $\delta$ 2<sup>+</sup> T cell activation was highly correlated within individuals (Fig. 1I). Plasma  
67 cytokines/chemokines IFN- $\gamma$ , IL-6, CCL-2, and TNF- $\alpha$  were induced following vaccination (Fig.  
68 S2D), consistent with data from non-human primates(11), and the degree of MAIT and V $\delta$ 2<sup>+</sup>  
69 T cell activation was correlated with changes in these innate cytokines/chemokines (Fig. 1J;  
70 Fig. S2E).

71 The mechanism of Ad vector-induced activation of MAIT cells was next investigated.  
72 Ad5 and ChAdOx1 displayed similar abilities to transduce PBMCs (Fig. S3A), and HLA-  
73 DR+CD11c+CD19-CD3<sup>-</sup> monocytes/cDCs were the major transduced population (83-98% of  
74 GFP<sup>+</sup> cells) (Fig. S3B, S3C). While Ad5 and ChAdOx1 both efficiently transduced  
75 monocytes/cDCs (Fig. 2A), Ad5 transduced only 1.5% of CD123<sup>+</sup> pDCs compared with 17.4%  
76 of CD123<sup>+</sup> pDCs transduced by ChAdOx1 (MOI=10<sup>3</sup> vp) (Fig. 2A), consistent with a prior report  
77 of poor pDC transduction by Ad5(12).

78 Given their efficient transduction, we sought to determine the role of monocytes in  
79 Ad vector-induced activation of MAIT cells. Depletion of monocytes significantly reduced  
80 expression of IFN- $\gamma$ , CD69, and granzyme B by MAIT cells following ChAdOx1 stimulation (Fig.  
81 2B; Fig. S4A). Consistent with prior studies on viruses(2, 3), MAIT cell activation by Ad vectors  
82 was independent of TCR signaling (Fig. S4B) -- suggesting a cytokine-mediated activation  
83 process. Depletion of monocytes abolished IL-18 secretion following vector stimulation (Fig.  
84 2C), and blockade of IL-18 signaling reduced MAIT cell IFN- $\gamma$ , CD69, and granzyme B  
85 production (Fig. 2D; Fig. S4C). Blocking IL-12 reduced only IFN- $\gamma$  production by MAIT cells (Fig.  
86 S4C), and blocking IL-15 had no effect. In contrast with ChAdOx1, Ad5 stimulation did not  
87 induce detectable levels of IL-18 or IL-12p70 (Fig S4D, S4E), consistent with the non-  
88 stimulatory nature of this vector. Direct inhibition of the Cathepsin B-NLRP3 inflammasome  
89 pathway(16) using four different pharmacologic approaches (Ca-074 Me, MCC950, elevated  
90 extracellular [K<sup>+</sup>], and Z-YVAD-FMK), significantly reduced expression of IFN- $\gamma$ , CD69, and  
91 granzyme B by MAIT cells (Fig. 2E; Fig. S5A-C), and production of IL-18 following ChAdOx1  
92 stimulation (Fig. 2F; Fig. S5D), similar to prior data examining IL-1 $\beta$ (17, 18). This effect was  
93 not due to altered transduction of PBMCs by ChAdOx1 (Fig. S5E).

94           Given the differential transduction of pDCs, the role of these cells in Ad vector-  
95 mediated activation of MAIT cells was investigated. Depletion of CD123+ pDCs resulted in a  
96 significant 67% reduction in IFN- $\gamma$  production by MAIT cells (Fig. 2G), and reduced IFN- $\alpha$  levels  
97 by >99% following ChAdOx1 stimulation (Fig. 2H). Inhibition of type I interferon signaling  
98 reduced IFN- $\gamma$  production by MAIT cells by 56-58% (Fig. 2I). Compared with ChAdOx1, Ad5  
99 induced negligible amounts of IFN- $\alpha$  (Fig. S6A, S6B), consistent with previous reports(11, 12).

100           We envisaged a model where monocyte-derived IL-18 and pDC-derived IFN- $\alpha$  were  
101 the minimal factors required to activate MAIT cells in response to ChAdOx1 stimulation.  
102 However, while IFN- $\alpha/\beta$  + IL-18 induced MAIT cell IFN- $\gamma$  in a PBMC culture, this was not seen  
103 using isolated MAIT cells (Fig. 3A), despite these cytokines upregulating CD69 on isolated  
104 MAIT cells (Fig. S7A). Depletion of monocytes from PBMCs reduced MAIT cell IFN- $\gamma$  production  
105 following IFN- $\alpha$  + IL-18 stimulation (Fig. S7B), and addition of monocytes rescued this (Fig.  
106 3B), indicating a monocyte-derived, IFN- $\alpha$ -dependent factor. The stimulatory factor was  
107 secreted, as either conditioned supernatant from IFN- $\alpha$ -treated monocytes (combined with  
108 IL-18), or provision of PBMCs across a transwell, significantly rescued IFN- $\gamma$  production by  
109 isolated MAIT cells (Fig. 3C; Fig. S7C). IFN- $\alpha$ -stimulated monocytes secreted multiple  
110 interferon-responsive chemokines (e.g. MCP-1/CCL2), as well as TNF- $\alpha$  (Fig. 3D; Fig. S7D).  
111 Addition of recombinant TNF- $\alpha$  or an anti-TNFR2 agonist to IFN- $\alpha$  + IL-18-stimulated isolated  
112 MAIT cells increased IFN- $\gamma$  production by >300% (from 4% to 16.5% and 17.6%, respectively;  
113 Fig. 3E; Fig. S7E). We confirmed the critical role of TNF- $\alpha$  as the presence of anti-TNF- $\alpha$   
114 antibody (adalimumab) during IFN- $\alpha$  + IL-18 stimulation of PBMCs inhibited IFN- $\gamma$  production  
115 by MAIT cells (Fig. S7F). The stimulatory capacity of supernatant from IFN- $\alpha$ -conditioned  
116 monocytes was also inhibited by the presence of adalimumab (Fig. S7G). TNF- $\alpha$  blockade  
117 using either adalimumab or recombinant TNFR2-Fc fusion protein (etanercept), but not a  
118 control anti- $\alpha 4\beta 7$  antibody (vedolizumab), inhibited IFN- $\gamma$  production by MAIT cells in  
119 response to ChAdOx1 (Fig. 3F; Fig. S7H). Depletion of monocytes reduced ChAdOx1-induced  
120 TNF- $\alpha$  production by 94% (Fig. 3G). Furthermore, Ad5 induced minimal TNF- $\alpha$  as compared  
121 with ChAdOx1 (Fig. S7I), consistent with the differential capacity of these two vectors to  
122 stimulate IFN- $\alpha$  production by pDCs (Fig. S6A).

123           V $\delta 2$ + T cells were activated by Ad vectors through similar mechanisms (Fig. S8A-G).  
124 Compiling the data, the activation of innate-like T cells in response to Ad vectors requires the



125 concerted action of IFN- $\alpha$ , TNF- $\alpha$ , and IL-18 (Fig. S9). These data extend prior reports of IFN-  
126  $\alpha$ -dependent activation of MAIT and V $\delta$ 2+ T cells by viruses(3, 19), by identifying a novel role  
127 for TNF- $\alpha$  as a necessary critical intermediary in this signaling pathway.

128 We next sought to determine the impact of MAIT cell activation on the induction of  
129 conventional T cell responses by ChAdOx1 immunization. C57BL/6J mice were immunized  
130 intramuscularly with ChAdOx1 or Ad5 at 10<sup>8</sup> IU, and MAIT cell activation in the spleen, liver,  
131 and inguinal LNs was measured on day 1 (Fig. S10A-C). ChAdOx1 induced substantial  
132 upregulation of CD69 and granzyme B on MAIT cells in the inguinal LNs, and to a lesser degree  
133 in the liver (Fig. 4A, 4B). Ad5 induced significantly less expression of CD69 and granzyme B. In  
134 mice, iNKT cells are the most abundant innate-like T cell population(20), and CD69 and  
135 granzyme B were also significantly upregulated on iNKT cells following ChAdOx1  
136 immunization, with Ad5 inducing less activation (Fig. S10D, S10E). These findings validate the  
137 use of a mouse model, as these data recapitulate the (differential) activation of MAIT cells by  
138 Ad vectors.

139 Having validated the model, we next addressed the role of MAIT cells in  
140 immunogenicity of Ad vector vaccines. Wildtype (WT) C57BL/6J and MR1 KO mice (Fig. S10F-  
141 H)(21) were immunized intramuscularly with 10<sup>8</sup> IU of ChAdOx1 expressing an optimized  
142 invariant chain-linked HCV antigen(22, 23), and HCV-specific immune responses were  
143 measured on day 16 post-immunization. Following vaccination, MR1 KO mice had significantly  
144 reduced frequencies of CD8 T cells that produced IFN- $\gamma$ , TNF- $\alpha$ , or both IFN- $\gamma$  and TNF- $\alpha$  in  
145 response to HCV peptides, as compared with WT mice (Fig. 4C-F). This functional defect  
146 appeared specific to the CD8 T cell compartment, as there was no significant reduction in the  
147 frequency of HCV-specific CD4 T cells following vaccination of MR1 KO mice (Fig. S10I). HCV-  
148 specific CD8 T cells from MR1 KO mice also showed reduced degranulation, as measured by  
149 CD107a (Fig. 4G), and these cells displayed impaired differentiation towards KLRG1+ effector  
150 cells (Fig. S10J).

151 In summary, MAIT cells are capable of sensing the diversity of the Ad vector-induced  
152 innate immune activation landscape (e.g. IFN- $\alpha$ , TNF- $\alpha$ , IL-18) and can integrate these signals  
153 to augment vaccine-induced adaptive immune responses. The blend of signals required to  
154 maximally trigger MAIT cells uncovered here includes a novel and critical pathway via IFN-  
155 dependent TNF- $\alpha$  release, relying on cross-talk between two distinct populations of

156 transduced cells, and varying between adenovirus serotypes. This full integration process is  
157 required for robust IFN- $\gamma$  production, which has been shown to be critical for MAIT cell-  
158 mediated protection from viral infection(4).

159 This non-redundant role for MAIT cells places them in a critical bridging position  
160 between innate and adaptive immunity, despite many potentially shared functions with other  
161 innate-like populations(9). These data, coupled with studies in the lung(4, 24, 25), support  
162 an emerging model that MAIT cells can function to orchestrate early events in T cell-mediated  
163 immunity. It is striking that activation of MAIT cells – an abundant human innate-like  
164 population – is tightly and mechanistically linked to the immunogenicity of adenovirus  
165 vectors, which have emerged as a potent platform for T cell immunogenicity in human clinical  
166 trials(26, 27). This knowledge can be harnessed to further improve the design and  
167 development of these – and potentially other – vaccines against infections and cancer.

168

#### 169 **References and Notes**

- 170 1. J. E. Ussher *et al.*, CD161<sup>++</sup> CD8<sup>+</sup> T cells, including the MAIT cell subset, are  
171 specifically activated by IL-12+IL-18 in a TCR-independent manner. *Eur J Immunol.* **44**,  
172 195–203 (2014).
- 173 2. L. Loh *et al.*, Human mucosal-associated invariant T cells contribute to antiviral  
174 influenza immunity via IL-18-dependent activation. *Proc Natl Acad Sci USA.* **113**,  
175 10133–10138 (2016).
- 176 3. B. van Wilgenburg *et al.*, MAIT cells are activated during human viral infections.  
177 *Nature Communications.* **7**, 11653 (2016).
- 178 4. B. V. Wilgenburg *et al.*, MAIT cells contribute to protection against lethal influenza  
179 infection in vivo. *Nature Communications.* **9**, 4706 (2018).
- 180 5. A. Vitelli *et al.*, Chimpanzee adenoviral vectors as vaccines – Challenges to move the  
181 technology into the fast lane. *Expert Review of Vaccines.* **0**, 1–22 (2017).
- 182 6. J.-X. Li *et al.*, Immunity duration of a recombinant adenovirus type-5 vector-based  
183 Ebola vaccine and a homologous prime-boost immunisation in healthy adults in  
184 China: final report of a randomised, double-blind, placebo-controlled, phase 1 trial.  
185 *Lancet Glob Health.* **5**, e324–e334 (2017).

- 186 7. L. Coughlan *et al.*, Heterologous Two-Dose Vaccination with Simian Adenovirus and  
187 Poxvirus Vectors Elicits Long-Lasting Cellular Immunity to Influenza Virus A in Healthy  
188 Adults. *EBIOM*. **29**, 146–154 (2018).
- 189 8. N. M. Provine *et al.*, Unique and Common Features of Innate-Like Human V $\delta$ 2+  $\gamma\delta$ T  
190 Cells and Mucosal-Associated Invariant T Cells. *Front Immunol*. **9**, 120–12 (2018).
- 191 9. M. Gutierrez-Arcelus *et al.*, Lymphocyte innateness defined by transcriptional states  
192 reflects a balance between proliferation and effector functions. *Nature*  
193 *Communications*. **10**, 687 (2019).
- 194 10. K. M. Quinn *et al.*, Antigen expression determines adenoviral vaccine potency  
195 independent of IFN and STING signaling. *J Clin Invest*. **125**, 1129–1146 (2015).
- 196 11. J. E. Teigler, M. J. Iampietro, D. H. Barouch, Vaccination with adenovirus serotypes 35,  
197 26, and 48 elicits higher levels of innate cytokine responses than adenovirus serotype  
198 5 in rhesus monkeys. *J Virol*. **86**, 9590–9598 (2012).
- 199 12. M. J. Johnson *et al.*, Type I IFN induced by adenovirus serotypes 28 and 35 has  
200 multiple effects on T cell immunogenicity. *J Immunol*. **188**, 6109–6118 (2012).
- 201 13. J. Alonso-Padilla *et al.*, Development of Novel Adenoviral Vectors to Overcome  
202 Challenges Observed With HAdV-5–based Constructs. *Mol Ther*. **24**, 6–16 (2015).
- 203 14. M. D. J. Dicks *et al.*, A Novel Chimpanzee Adenovirus Vector with Low Human  
204 Seroprevalence: Improved Systems for Vector Derivation and Comparative  
205 Immunogenicity. *PLoS ONE*. **7**, e40385 (2012).
- 206 15. S. F. Farina *et al.*, Replication-Defective Vector Based on a Chimpanzee Adenovirus. *J*  
207 *Virol*. **75**, 11603–11613 (2001).
- 208 16. V. Hornung *et al.*, Silica crystals and aluminum salts activate the NALP3  
209 inflammasome through phagosomal destabilization. *Nature Immunology*. **9**, 847–856  
210 (2008).
- 211 17. A. U. Barlan, T. M. Griffin, K. A. McGuire, C. M. Wiethoff, Adenovirus membrane  
212 penetration activates the NLRP3 inflammasome. *J Virol*. **85**, 146–155 (2011).
- 213 18. D. A. Muruve *et al.*, The inflammasome recognizes cytosolic microbial and host DNA  
214 and triggers an innate immune response. *Nature*. **452**, 103–107 (2008).
- 215 19. C.-Y. Tsai *et al.*, Type I IFNs and IL-18 regulate the antiviral response of primary  
216 human  $\gamma\delta$  T cells against dendritic cells infected with Dengue virus. *J Immunol*. **194**,  
217 3890–3900 (2015).

- 218 20. L. C. Garner, P. Klenerman, N. M. Provine, Insights Into Mucosal-Associated Invariant  
219 T Cell Biology From Studies of Invariant Natural Killer T Cells. *Front Immunol.* **9**, 911–  
220 25 (2018).
- 221 21. E. Treiner *et al.*, Selection of evolutionarily conserved mucosal-associated invariant T  
222 cells by MR1. *Nature.* **422**, 164–169 (2003).
- 223 22. A. von Delft *et al.*, The generation of a simian adenoviral vectored HCV vaccine  
224 encoding genetically conserved gene segments to target multiple HCV genotypes.  
225 *Vaccine.* **36**, 313–321 (2018).
- 226 23. P. J. Holst *et al.*, MHC class II-associated invariant chain linkage of antigen  
227 dramatically improves cell-mediated immunity induced by adenovirus vaccines. *J*  
228 *Immunol.* **180**, 3339–3346 (2008).
- 229 24. A. Meierovics, W.-J. C. Yankelevich, S. C. Cowley, MAIT cells are critical for optimal  
230 mucosal immune responses during in vivo pulmonary bacterial infection. *Proc Natl*  
231 *Acad Sci USA.* **110**, E3119–28 (2013).
- 232 25. A. I. Meierovics, S. C. Cowley, MAIT cells promote inflammatory monocyte  
233 differentiation into dendritic cells during pulmonary intracellular infection. *J Exp Med.*  
234 **59**, jem.20160637–18 (2016).
- 235 26. J. E. Ledgerwood *et al.*, Chimpanzee Adenovirus Vector Ebola Vaccine. *N Engl J Med.*  
236 **376**, 928–938 (2017).
- 237 27. D. H. Barouch *et al.*, Evaluation of a mosaic HIV-1 vaccine in a multicentre,  
238 randomised, double-blind, placebo-controlled, phase 1/2a clinical trial (APPROACH)  
239 and in rhesus monkeys (NHP 13-19). *Lancet.* **392**, 232–243 (2018).
- 240 28. R. D. Antrobus *et al.*, Clinical Assessment of a Novel Recombinant Simian Adenovirus  
241 ChAdOx1 as a Vectored Vaccine Expressing Conserved Influenza A Antigens. *Mol Ther.*  
242 **22**, 668–674 (2013).
- 243 29. S. Colloca *et al.*, Vaccine vectors derived from a large collection of simian  
244 adenoviruses induce potent cellular immunity across multiple species. *Sci Transl Med.*  
245 **4**, 115ra2 (2012).
- 246 30. N. M. Provine *et al.*, Immediate Dysfunction of Vaccine-Elicited CD8+ T Cells Primed in  
247 the Absence of CD4+ T Cells. *J Immunol.* **197**, 1809–1822 (2016).
- 248 31. N. M. Provine *et al.*, Longitudinal Requirement for CD4+ T Cell Help for Adenovirus  
249 Vector-Elicited CD8+ T Cell Responses. *J Immunol.* **192**, 5214–5225 (2014).

- 250 32. M. Murata *et al.*, Novel epoxysuccinyl peptides. Selective inhibitors of cathepsin B, in  
251 vitro. *FEBS Lett.* **280**, 307–310 (1991).
- 252 33. R. C. Coll *et al.*, A small-molecule inhibitor of the NLRP3 inflammasome for the  
253 treatment of inflammatory diseases. *Nat Med.* **21**, 248–255 (2015).
- 254 34. R. Muñoz-Planillo *et al.*, K<sup>+</sup> Efflux Is the Common Trigger of NLRP3 Inflammasome  
255 Activation by Bacterial Toxins and Particulate Matter. *Immunity.* **38**, 1142–1153  
256 (2013).
- 257 35. M. Garcia-Calvo *et al.*, Inhibition of human caspases by peptide-based and  
258 macromolecular inhibitors. *J Biol Chem.* **273**, 32608–32613 (1998).

259

## 260 **Acknowledgements**

261 We would like to thank: Stephanie Slevin and Helen Ferry for assistance with flow cytometry  
262 and panel design, Carl-Philipp Hackstein and Christian Willberg for critical discussions,  
263 Mariolina Salio and Vincenzo Cerundolo for provision of MR1 KO mice, Marilù Esposito,  
264 Hussein Al-Mossawi, Lian Ni Lee, and Timothy Donnison for provision of reagents, the NIH  
265 Tetramer Facility for provision of MR1 and CD1d tetramers, and all of the volunteers for  
266 participation in the trial and donation of blood samples.

267

## 268 **Funding**

269 NMP is supported by an Oxford-UCB Postdoctoral Fellowship.

270 AA is supported by a Wellcome Clinical Training Fellowship [216417/Z/19/Z].

271 LCG is supported by a Wellcome PhD Studentship [109028/Z/15/Z].

272 MEBF is supported by an Oxford-Celgene Doctoral Fellowship.

273 CR is supported by the NIHR Biomedical Research Centre and is a Jenner Institute Investigator.

274 AJP is supported by the NIHR Oxford Biomedical Research Centre and is an NIHR Senior  
275 Investigator.

276 PK is supported by the Wellcome Trust [WT109965MA], the Medical Research Council (STOP-  
277 HCV), an NIHR Senior Fellowship, and the NIHR Biomedical Research Centre (Oxford).

278 The ChAdOx1-MenB.1 clinical trial is funded by the MRC (DPFS).

279 The views expressed are those of the authors and not necessarily those of the NHS, the NIHR  
280 or the Department of Health.

281

282 **Author contributions**

283 NMP and PK designed the project.

284 NMP, CD, CSR, EB, AJP, and PK designed the experiments.

285 NMP, AA, LCG, CD, CH, MEBF, LSR performed the experiments.

286 LSR, SC, BO, MR, SC, AF, CR, EB, and AJP provided samples and reagents.

287 All authors contributed to the writing and editing of the manuscript.

288

289 **Competing interests**

290 Authors declare no competing interests.

291

292 **Data Availability**

293 All primary data available upon request.

294

295 **Supplementary Materials**

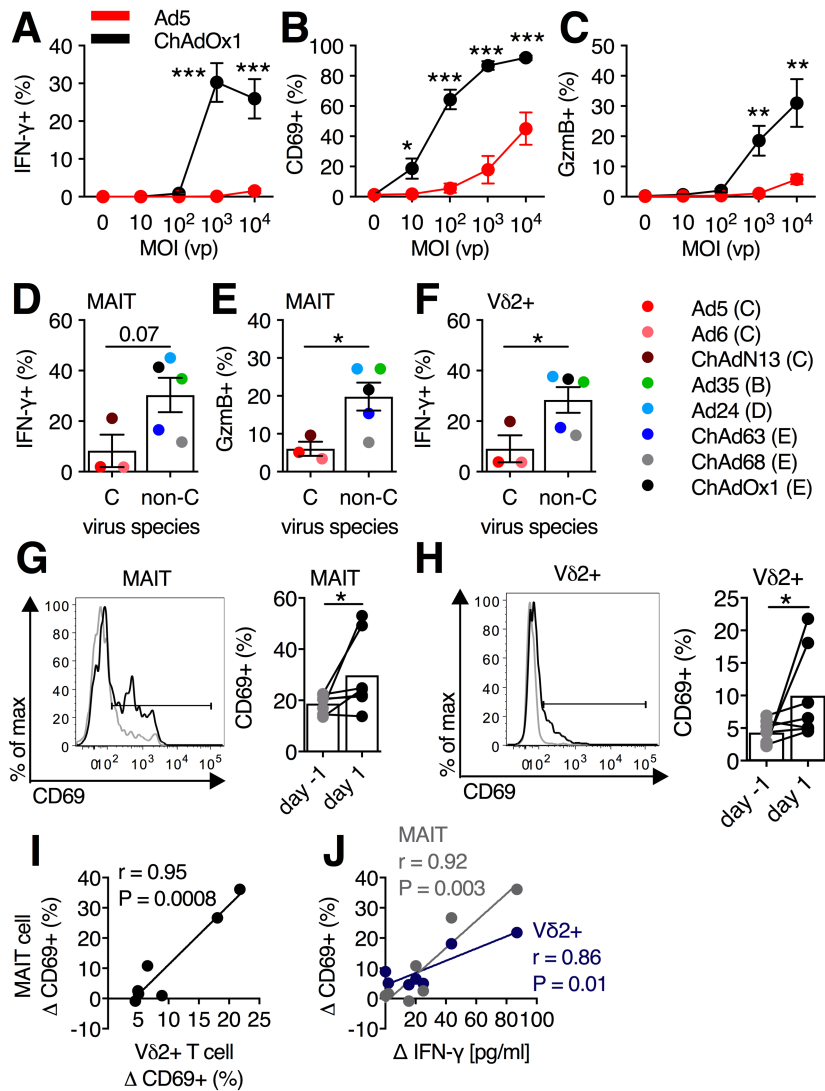
296 Materials and Methods

297 Figs. S1 to S10

298 References (28-35)

299

300 **Figures and legends**



301

302 **Figure 1. *In vitro* and *in vivo* activation of human MAIT and V $\delta$ 2+ T cells by adenovirus**

303 **vectors. (A-C)** PBMCs (N=9) were stimulated with Ad5 or ChAdOx1 at increasing MOIs (0 to

304 10<sup>4</sup> vp), and IFN- $\gamma$  (A), CD69 (B), and granzyme B (GzmB) (C) expression was measured on

305 MAIT cells (CD161++V $\alpha$ 7.2+ T cells) after 24 h. (D-F) PBMCs were stimulated with MOI=10<sup>3</sup>

306 vp of the indicated vector (species in parentheses) for 24 h (N=5 per vector). Average IFN- $\gamma$

307 (D) or GzmB (E) production by MAIT cells, and IFN- $\gamma$  production by V $\delta$ 2+ T cells (F) in response

308 to stimulation with the indicated vector. (G-J) Healthy human volunteers (N=7) were

309 immunized with a 5x10<sup>10</sup> vp dose of ChAdOx1 expressing a *N. meningitidis* group B antigen

310 (MenB.1). Expression of CD69 on MAIT (MR1/5-OP-RU++ T cells) (G) and V $\delta$ 2+ T cells (H) in

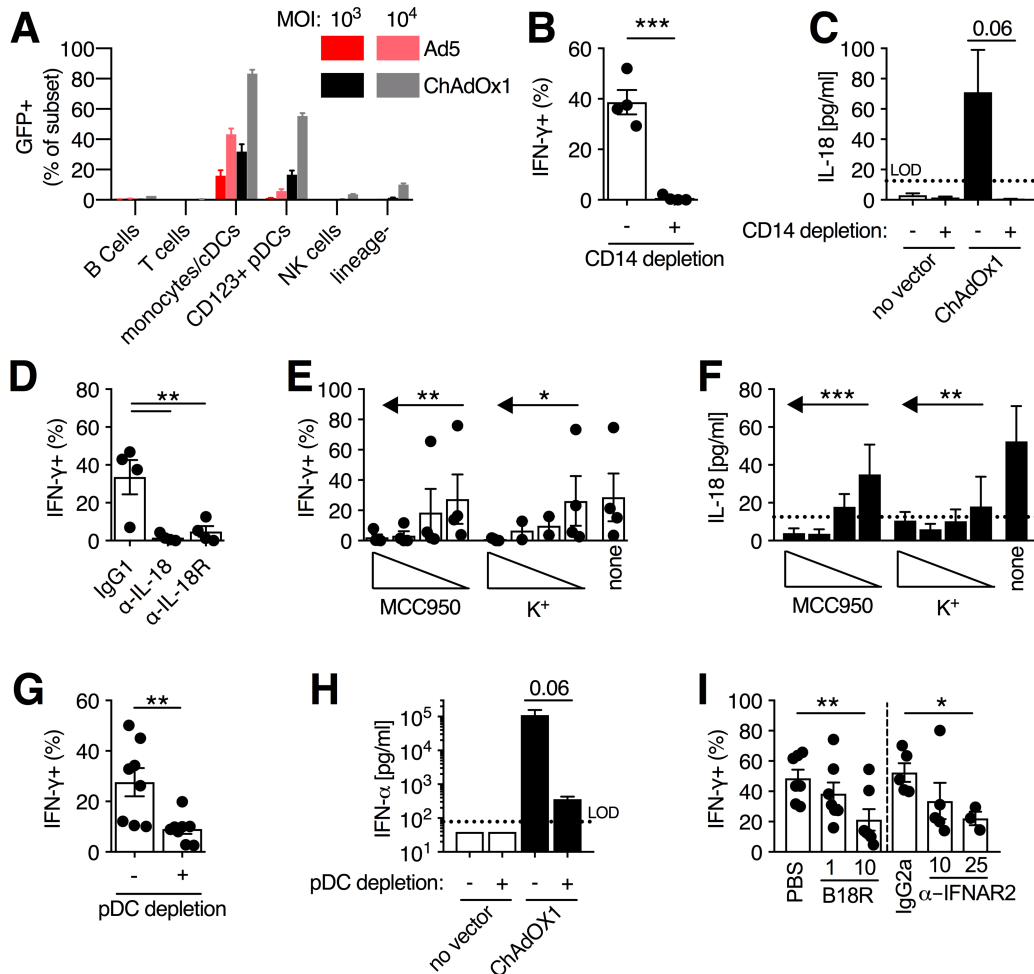
311 peripheral blood one day pre- and one day post-immunization. (I) Pearson correlation of

312 change in CD69 expression on MAIT cells and V $\delta$ 2+ T cells following vaccination. (J) Pearson

313 correlation of change in plasma IFN- $\gamma$  level following vaccination with the change in



314 expression of CD69 on MAIT cells and V $\delta$ 2+ T cells. \*, P<0.05; \*\*, P<0.01; \*\*\*, P<0.001.  
315 Unpaired T test (**A-F**) or Wilcoxon rank-sum test (**G,H**). Symbols indicate average response of  
316 5 donors for each vector (**D-F**) and individual donors (**G-J**), and group mean ( $\pm$  SEM) are  
317 shown.  
318  
319



320

321 **Figure 2. Activation of MAIT cells by adenovirus vectors requires monocyte-derived IL-18**

322 **and pDC-derived IFN- $\alpha$ .** (A) Fresh human PBMCs (N=3) were stimulated for 24 h with either

323 Ad5 or ChAdOx1 at MOI=10<sup>3</sup> vp, and the fraction of each PBMC immune subset that was GFP+

324 was assessed. (B) PBMCs were depleted of CD14+ monocytes or left untreated as a control

325 (N=4), and IFN- $\gamma$  expression was measured on MAIT cells (CD161++V $\alpha$ 7.2+ T cells) after 24 h

326 stimulation with ChAdOx1 (MOI=10<sup>3</sup> vp). (C) Concentration of IL-18 in cell culture

327 supernatants of whole PBMCs (N=5) or CD14-depleted PBMCs (N=4) 24 h after stimulation

328 with ChAdOx1. (D) PBMCs (N=4) were treated with either anti-IL-18 or anti-IL-18R antibodies

329 (10  $\mu$ g/ml) immediately prior to stimulation with ChAdOx1 (MOI=10<sup>3</sup> vp). IFN- $\gamma$  production by

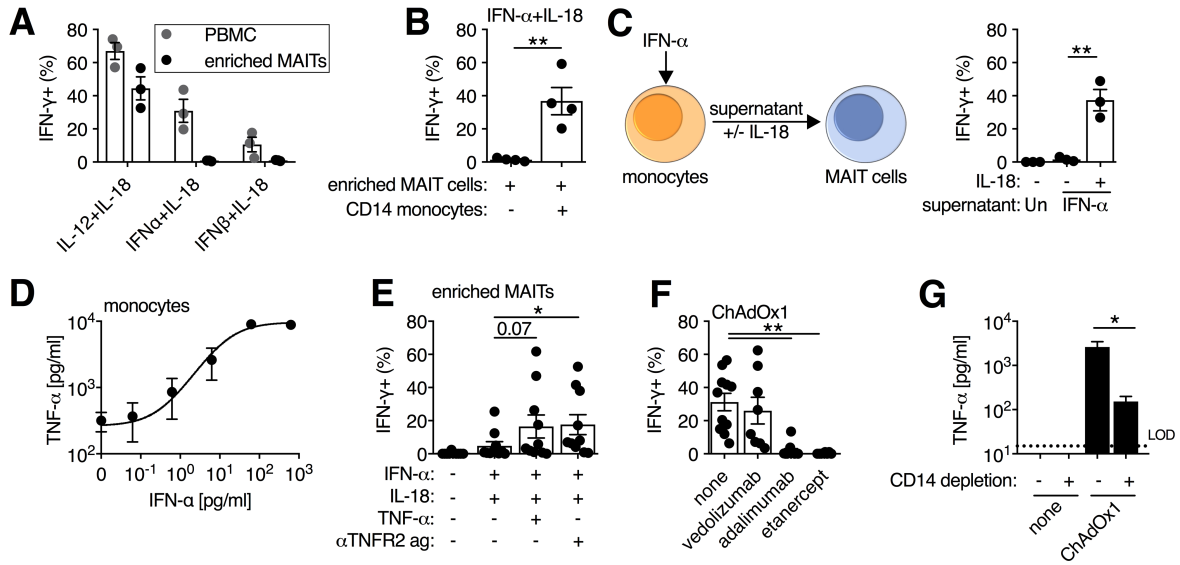
330 MAIT cells was measured after 24 h. (E,F) The NLRP3 inhibitors (MCC950 [0.01-10  $\mu$ M] and

331 extracellular K<sup>+</sup> [5-30 mM]) were added immediately prior to stimulation of PBMCs (N=4)

332 with ChAdOx1. After 24 h, IFN- $\gamma$  production by MAIT cells (E) and concentration of IL-18 in the

333 cell culture supernatant (F) was assessed (N=4). (G,H) PBMCs were depleted of CD123+ pDCs

334 or left untreated as a control (N=8), and IFN- $\gamma$  expression on MAIT cells (**G**) or concentration  
335 of IFN- $\alpha$  in the cell culture supernatant (**H**) was measured after 24 h. (**I**) PBMCs were  
336 stimulated with ChAdOx1 (MOI=10<sup>3</sup> vp) and B18R (1 or 10  $\mu$ g/ml) or anti-IFNAR2 antibody (10  
337 or 25  $\mu$ g/ml) were added immediately prior to vector addition. IFN- $\gamma$  expression was  
338 measured on MAIT-cells after 24 h. N=7 for B18R, and N=5 for anti-IFNAR2 antibody at 10  
339  $\mu$ g/ml and N=3 for 25  $\mu$ g/ml. \*, P<0.05; \*\*, P<0.01; \*\*\*, P<0.001. Unpaired T test (**B,C,G,H**),  
340 repeated-measures one-way ANOVA with Dunnett Correction (**D,I**), repeated-measures one-  
341 way ANOVA with test for linear trend (**E,F**). Symbols indicate individual donors, and mean  $\pm$   
342 SEM are shown.  
343  
344



345

346

**Figure 3. IFN-α acts directly and indirectly through the induction of TNF-α to activate MAIT**

347

**cells. (A)** Unfractionated PBMCs or enriched MAIT cells (positive selection by CD8

348

MicroBeads) were stimulated for 24 h with the indicated cytokines (50 ng/ml), and IFN-γ

349

expression was measured on MAIT cells (CD161++Vα7.2+ T cells) after 24 h (N=3). **(B)**

350

Enriched MAIT cells with or without CD14+ monocytes (positive selection by CD14

351

MicroBeads) were stimulated with IFN-α and IL-18 (50 ng/ml). IFN-γ production by MAIT

352

cells was measured after 24 h (N=4). **(C)** Purified monocytes (N=3) were stimulated for with IFN-α

353

(50 ng/ml), or left untreated, and after 24 h supernatants were transferred to autologous

354

enriched MAIT cells with or without the addition of IL-18 (50 ng/ml). IFN-γ production by MAIT

355

cells was measured after 24 h. **(D)** CD14-purified monocytes (N=3) were stimulated with

356

increasing concentrations of IFN-α and TNF-α concentration in the cell culture supernatant

357

was measured after 24 h. **(E)** Enriched MAIT cells (N=10) were stimulated with IFN-α and IL-

358

18 ± TNF-α (50 ng/ml) or anti-TNFR2 agonist antibody (2.5 μg/ml), and IFN-γ production by

359

MAIT cells was measured at 24 h. **(F)** PBMCs were stimulated with ChAdOx1 (MOI=10<sup>3</sup> vp)

360

and vedolizumab (anti-α4β7 integrin antibody, N=8), adalimumab (anti-TNF-α antibody,

361

N=11), or etanercept (TNFR2-Fc fusion protein, N=8) (10 μg/ml) were added immediately

362

prior to vector addition. IFN-γ production by MAIT cells was measured after 24 h. **(G)**

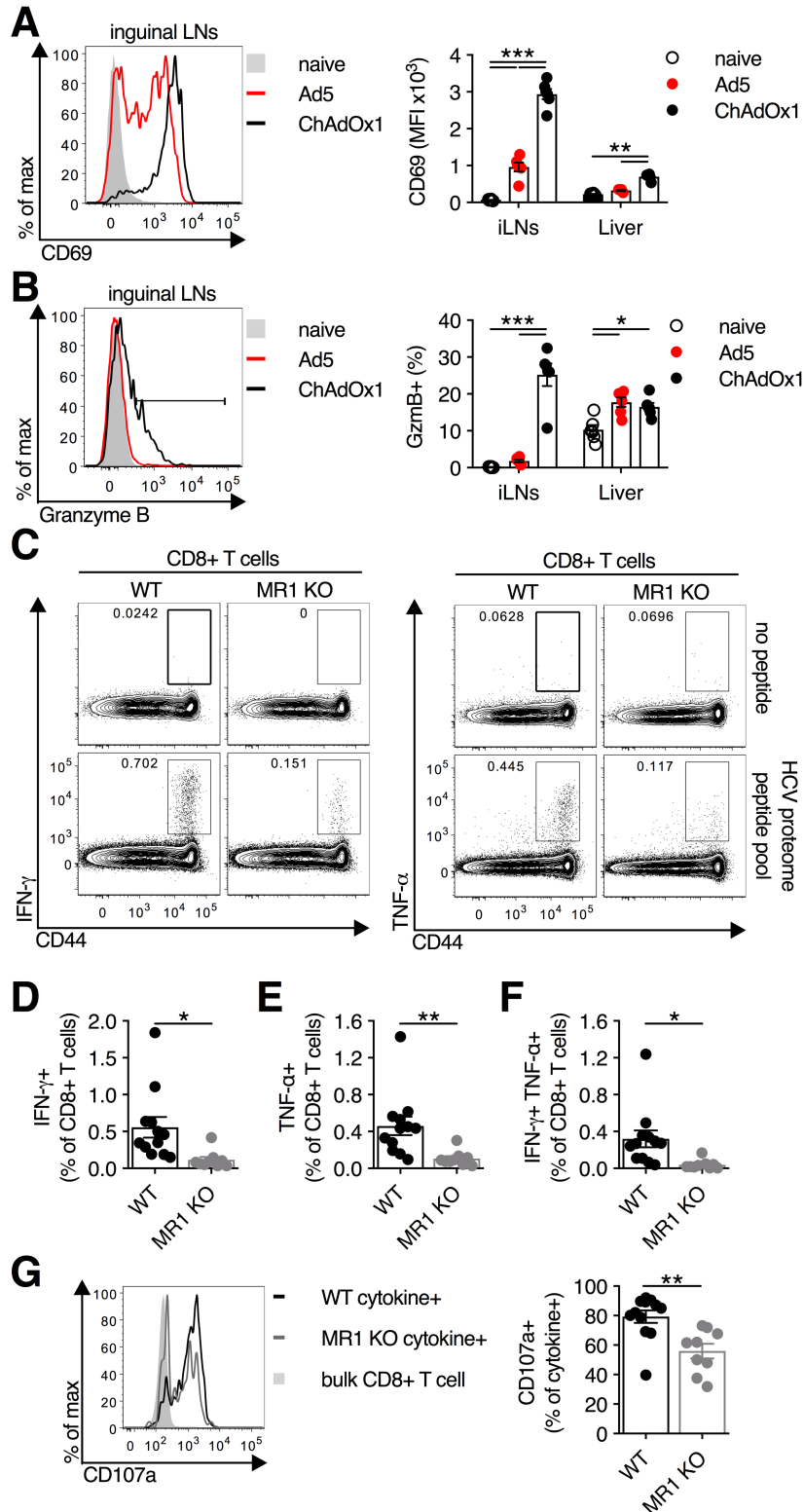
363

Concentration of TNF-α in cell culture supernatants of whole PBMCs or CD14-depleted PBMCs

364

24 h after stimulation with ChAdOx1 (MOI=10<sup>3</sup> vp; N=4). \*, P<0.05; \*\*, P<0.01. Unpaired T

365 test **(B,C,G)**, repeated-measures one-way ANOVA with Dunnett Correction **(E,F)**. Symbols  
366 indicate individual donors, and mean  $\pm$  SEM are shown.



367

368 **Figure 4. MAIT cell-deficient mice have impaired vaccine-induced CD8 T cell responses**

369 **following ChAdOx1 immunization. (A,B)** C57BL/6J mice (N=6 per group) were immunized

370 intramuscularly with 10<sup>8</sup> IU of Ad5 or ChAdOx1 expressing GFP, and one day post-

371 immunization, expression of CD69 **(A)** and granzyme B (GzmB) **(B)** was measured on MAIT

372 cells (MR1/5-OP-RU+ T cells) isolated from inguinal LNs and liver. Data are representative of  
373 two independent experiments. **(C-G)** C57BL/6J (N=12) or MR1 KO (N=9) mice were immunized  
374 intramuscularly with  $10^8$  IU of ChAdOx1 expressing HCV-GT1-6\_D\_TM-li+L transgene, and on  
375 day 16 post-immunization splenocytes were collected. Representative flow cytometry plots  
376 **(C)** and group averages of IFN- $\gamma$  production **(D)**, TNF- $\alpha$  production **(E)**, or dual production of  
377 IFN- $\gamma$  and TNF- $\alpha$  **(F)** by CD8 T cells following 5 h restimulation with an overlapping peptide pool  
378 of the HCV genotype 1b proteome. **(G)** Representative flow cytometry plots and group  
379 averages of CD107a expression on cytokine-producing CD8 T cells following peptide  
380 restimulation. \*, P<0.05; \*\*, P<0.01; \*\*\*, P<0.001. One-way ANOVA with Sidak correction for  
381 multiple comparisons **(A,B)**, Unpaired T test **(D-G)**. Symbols indicate individual animals, and  
382 mean  $\pm$  SEM are shown.



1 Supplementary Material for

2

3 **Activation of MAIT cells plays a critical role in viral vector vaccine immunogenicity**

4

5 Nicholas M. Provine\*, Ali Amini, Lucy C. Garner, Christina Dold, Claire Hutchings, Michael E.B.  
6 FitzPatrick, Laura Silva Reyes, Senthil Chinnakannan, Blanche Oguti, Meriel Raymond, Stefania  
7 Capone, Antonella Folgori, Christine S. Rollier, Eleanor Barnes, Andrew J. Pollard, Paul  
8 Klenerman\*

9

10 \* Corresponding authors: [nicholas.provine@ndm.ox.ac.uk](mailto:nicholas.provine@ndm.ox.ac.uk); [paul.klenerman@ndm.ox.ac.uk](mailto:paul.klenerman@ndm.ox.ac.uk)

11

12 **This PDF file includes:**

13 Materials and Methods

14 Figs. S1 to S10

15 References (28-35)

16

## 17 **Materials and Methods**

18 **Vectors and viruses.** E1/E3-deleted replication-incompetent recombinant Ad5-GFP (VP:PFU  
19 ratio batch 1: 34, batch 2: 15, batch 3: 21) , ChAdOx1-GFP (VP:PFU ratio batch 1: 118, batch  
20 2: 13, batch 3: 78, batch 4: 73), ChAdOx1-HCV-GT1-6\_D\_TM-Ii+L(22) (VP:PFU ratio 95), and  
21 ChAd63-GFP (VP:PFU ratio 107) adenovirus vectors were produced by the Jenner Institute  
22 Viral Vector Core Facility at the University of Oxford, as previously described(14). ChAdOx1-  
23 MenB.1 (VP:PFU ratio 96) was produced at the Clinical Biomanufacturing Facility at the  
24 University of Oxford as previously described(28). E1/E3-deleted replication-incompetent  
25 recombinant Ad6 (VP:PFU ratio 95), ChAdN13 (VP:PFU ratio not calculated), Ad24 (VP:PFU  
26 ratio not calculated), Ad35 (VP:PFU ratio 124), and ChAd68 (AdC68; VP:PFU ratio 100)  
27 adenovirus vectors were produced by Nouscom, SRL (Rome, Italy), as previously  
28 described(29). Briefly, vectors were propagated in HEK293, except for ChAdOx1-MenB.1  
29 which was propagated in PER.C6 cells, and isolated by CsCl<sub>2</sub> ultracentrifugation.

30 **Human PBMCs and isolation of cell populations.** Fresh blood from healthy human volunteers  
31 was collected in EDTA-coated Vacutainer tubes (BD Biosciences) under the “Gastrointestinal  
32 Illness in Oxford: prospective cohort for outcomes, treatment, predictors and biobanking”  
33 (Ref: 11/YH/0020) ethics, or blood from anonymized healthy donors was collected from the  
34 NHS Blood and Transplant Service. Peripheral blood mononuclear cells (PBMCs) were isolated  
35 by density gradient centrifugation, as previously described(8). Briefly, PBS was used to dilute  
36 blood prior to layering over Lymphoprep (Axis-Shield or STEMCELL Technologies). Samples  
37 were centrifuged at 973 *g* for 30 minutes and allowed to decelerate without the brake. The  
38 PBMC layer was collected and washed once in R10 media [RPMI-1640 (Lonza) + 10% FBS  
39 (Sigma Aldrich) + 1% penicillin/streptomycin (Sigma-Aldrich)]. Red blood cells were lysed by  
40 incubation of the cell pellet in an 1x Ammonium-Chloride-Potassium (ACK) solution for <5  
41 min. Cells were washed again in R10, and either used immediately or stored in liquid nitrogen.

42 CD8 MicroBeads (Miltenyi Biotec) were used to generate enriched MAIT-cell  
43 populations. CD14 MicroBeads and CD123 MicroBeads (Miltenyi Biotec) were used to deplete  
44 monocytes and plasmacytoid DCs (pDCs), respectively. All kits were used as per the  
45 manufacturer’s instructions.

46 **Vaccinated human volunteers.** PBMCs and plasma were collected from healthy volunteers  
47 aged 18-50 enrolled in the clinical trial ISRCTN trial number: ISRCTN46336916. Briefly,

48 volunteers received a homologous prime-boost of  $5 \times 10^{10}$  vp of ChAdOx1-MenB.1 at a 6-  
49 month interval. Samples were collected prior to the second immunization and 1 day after.

50 **Mice and tissue processing.** JAX™ C57BL/6J mice (aged 6-10 weeks) were purchased from  
51 Charles River. MR1 KO mice(21) (kindly provided by Mariolina Salio and Vincenzo Cerundolo,  
52 University of Oxford) were bred in house and used at 6-10 weeks of age. Sex and age were  
53 matched between groups. All animals were housed in specific pathogen-free conditions at  
54 the Biomedical Services Building (University of Oxford) or the Wellcome Centre for Human  
55 Genetics (University of Oxford). All work was performed under UK Home Office license PPL  
56 30/3293 or 30/3386 in accordance with the UK Animal (Scientific Procedures) Act 1986. All  
57 work was performed by trained and licensed individuals.

58 Animals were immunized intramuscularly in the hind legs with  $10^8$  infectious units (IU)  
59 of Ad5-GFP, ChAdOx1-GFP, or ChAdOx1-HCV-GT1-6\_D\_TM-Ii+L, as previously described(22).  
60 Spleen and lymph nodes were processed as described previously(30). Briefly, tissue was  
61 dissociated through a 70  $\mu$ m filter and washed with R10 media. Red blood cells were lysed,  
62 as needed, with 1x ACK solution for <5 min, and cells were washed an additional time with  
63 R10 media before downstream applications. Liver tissue was processed as described  
64 previously(31). Briefly, liver tissue was ground through a 70  $\mu$ m filter, and washed once with  
65 R10 media. Liver mononuclear cells (MNCs) were isolated on a 35%-70% discontinuous Percoll  
66 (GE Healthcare) gradient by centrifugation at 741 *g* for 20 min and deceleration was without  
67 the brake. The MNC layer was collected, samples were washed once with R10 media, and  
68 residual red blood cells were lysed with 1x ACK solution for <5 min. After a final wash with  
69 R10 media, liver MNCs were used for downstream applications.

70 **Genotyping.** Genotyping of MR1 KO mice was performed by PCR and gel electrophoresis, as  
71 previously described(21). DNA was extracted from splenocytes using the Qiagen DNeasy  
72 Blood and Tissue Extraction kit per the manufacturer's instructions. For testing of wildtype  
73 *Mr1* the MR1 5' 8763-8783 (AGC TGA AGT CTT TCC AGA TCG) and MR1 9188-9168 rev (ACA  
74 GTC ACA CCT GAG TGG TTG) primers were used. For mutant *Mr1* the MR1 5' 8763-8783 (AGC  
75 TGA AGT CTT TCC AGA TCG) and MR1 10451-10431 (GAT TCT GTG AAC CCT TGC TTC) primers  
76 were used. Primers (Sigma-Aldrich) were used at 10  $\mu$ M and QuantiFast SYBR Green  
77 Mastermix (Qiagen) was used. Thermocycler conditions were: Step 1: 95 °C for 5 min, Step 2:  
78 94 °C for 30 sec, Step 3: 60 °C for 30 sec, Step 4: 72 °C for 30 sec, Step 5: repeat Step 2-4 35x,

79 Step 6: 72 °C for 5 Min, Step 7: hold at 22 °C. PCR products were run on a 2% Agarose gel and  
80 imaged on a GelDoc-It (UVP Imaging).

81 ***In vitro* MAIT and Vδ2+ T cell stimulation assays.** For *in vitro* stimulation of human PBMCs  
82 with Ad vectors, fresh PBMCs were used. For *in vitro* stimulation of human PBMCs with  
83 cytokines, fresh or freeze-thawed PBMCs were used with equivalent outcomes. For Ad vector  
84 stimulations, a previously described protocol(11) was used with slight modifications. 10<sup>6</sup>  
85 whole PBMCs or cell subset-depleted PBMCs were added to a 96 well U-bottom plate. Ad-  
86 vectors were added at an MOI of 10<sup>3</sup> vp, unless indicated otherwise. If applicable, inhibitory  
87 compounds or recombinant cytokines were added immediately prior to addition of the  
88 vector. Samples were mixed and incubated at 37 °C in 5% CO<sub>2</sub>.

89 For cytokine stimulations, a previously-described protocol(1) was used with slight  
90 modifications. Briefly, 10<sup>6</sup> whole PBMCs or cell subset-depleted PBMCs were added to a 96  
91 well U-bottom plate, and for isolated CD14+ monocytes and enriched MAIT-cells, 1-2x10<sup>5</sup> cells  
92 were used. For the transwell assay, a 0.3 μm 96 well transwell plate (Corning) was used. 2x10<sup>5</sup>  
93 enriched MAIT-cells were added to the bottom chamber, and 10<sup>6</sup> PBMCs were added to the  
94 top chamber. IFN-α2A (Sigma-Aldrich), IL-12p70 (R&D Systems), IL-18 (R&D Systems), and  
95 TNF-α (R&D Systems) were all used at a final concentration of 50 ng/ml. Anti-TNFR2 agonist  
96 antibody (clone: MR2-1, Hycult Biotech) was used at a concentration of 2.5 μg/ml. If  
97 applicable, inhibitory compounds were added immediately prior to addition of cytokines.  
98 Samples were mixed and incubated at 37 °C in 5% CO<sub>2</sub>.

99 For measurements of MAIT and Vδ2+ T cell activation, Brefeldin A (final concentration  
100 of 5 μg/ml; BioLegend) was added after 20 h, and samples were collected after an additional  
101 4 h incubation (24 h total stimulation time). For experiments where cytokine secretion or  
102 characteristics of cell transduction were assessed, Brefeldin A was not added and samples  
103 were collected after 24 h.

104 **Blocking and inhibitory reagents.** The following reagents were used in the above-described  
105 *in vitro* stimulation assays: mouse IgG1 isotype control antibody (Clone: MOPC-21,  
106 BioLegend), mouse IgG2a isotype control antibody (clone: MOPC-173, BioLegend), anti-MR1  
107 antibody (clone: 26.5, BioLegend), anti-IL-12p70 antibody (clone: 24910, R&D Systems), anti-  
108 IL-15 antibody (clone: 34559, R&D Systems), anti-IL-18 antibody (clone: 125-2H, R&D  
109 Systems), anti-IL-18Rα antibody (clone: 70625, R&D Systems), anti-IFNAR2 (clone: MMHAR-

110 2, Merck Chemicals), B18R (eBioscience), mevastatin (Merck Chemicals), CA-074-Me(32)  
111 (Merck Chemicals), MCC950(33) (Sigma-Aldrich), elevated extracellular K<sup>+</sup> ion  
112 concentration(34) (KCl, Sigma-Aldrich) , Z-YVAD-FMK(35) (R&D Systems), vedolizumab (anti-  
113  $\alpha 4\beta 7$  integrin antibody; Takeda Pharmaceuticals), adalimumab (anti-TNF- $\alpha$  antibody; AbbVie  
114 Inc), etanercept (TNFR2-Fc fusion protein; Pfizer; A kind gift of Dr. Hussein Al-Mossawi,  
115 University of Oxford).

116 **Quantification of cytokines and chemokines.** For quantification of cell culture supernatant,  
117 the following ELISA kits were used: Human TNF- $\alpha$  Quantikine ELISA kit (R&D Systems), IL-18  
118 Human ELISA Kit (MBL International), Human IL-12p70 Quantikine ELISA kit (R&D Systems),  
119 and VeriKine Human IFN- $\alpha$  Multi-Subtype ELISA Kit (PBL Assay Science) as per the  
120 manufacturer's instructions. All data were collected on a FLUOstar OPTIMA plate reader  
121 (BMG LABTECH). For multiplex analysis of IFN- $\alpha$ -stimulated monocytes the Proteome Profiler  
122 Human XL Cytokine Array Kit (R&D Systems) was used as per the manufacturer's instructions,  
123 and the membrane was developed for 10 minutes on an SRX-101A Film Processor (Konica  
124 Corporation). For analysis of plasma cytokines in vaccinated human volunteers, the  
125 LEGENDplex Human Inflammation Panel (13-plex) (BioLegend) was used per the  
126 manufacturer's instructions. For all assays, samples were diluted as appropriate to fall within  
127 the dynamic range of the assay. Samples were freeze-thawed a maximum of one time.

128 **MR1 and CD1d tetramer staining in mice and humans.** Human and murine MR1/5-OP-RU  
129 and MR1/6-FP, and murine CD1d/PBS-57 and CD1d/unloaded tetramers were provided by  
130 the NIH Tetramer Facility (Emory University). Tetramers were generated using Phycoerythrin  
131 (PE)-Streptavidin and Brilliant Violet 421-Streptavidin (BioLegend) following the NIH Tetramer  
132 Facility's guidelines. All tetramer staining was performed for 40 min at room temperature,  
133 and staining was performed in 50  $\mu$ l of FACS buffer (PBS + 0.05% BSA + 1% EDTA). Following  
134 tetramer staining, samples were washed twice in FACS buffer, and used for further staining  
135 described below.

136 **Surface and intracellular flow cytometry staining of human PBMCs.** For activation of MAIT  
137 and V $\delta$ 2<sup>+</sup> T cells, if MR1 tetramer staining was performed, it was done as above. Surface  
138 staining was performed using fixable live/dead vital dye (Life Technologies) for 15 min at 4 °C.  
139 After surface staining, samples were washed two times in FACS buffer, and cells were fixed  
140 and permeabilized for 20 min at 4 °C using Cytofix/Cytoperm (BD Biosciences). Samples were

141 subsequently washed two times in Perm/Wash buffer (BD Biosciences). Intracellular staining  
142 was performed for 30 min at 4 °C. The following antibodies were used in Perm/Wash buffer:  
143 anti-CD161 (clone: 191B8, Miltenyi Biotec), -CD69 (clone: FN50, BioLegend), -V $\alpha$ 7.2 TCR  
144 (clone: 3C10, BioLegend), -V $\delta$ 2 TCR (clone: B6, BioLegend), -CD3 $\epsilon$  (clone: OKT3 or UCHT1,  
145 BioLegend or BD Biosciences), -IFN- $\gamma$  (clone: B27, BioLegend and BD Biosciences), and -  
146 granzyme B (clone: GB11, BD Biosciences). Following intracellular staining, samples were  
147 washed two additional times in Perm/Wash buffer, and stored in FACS buffer at 4 °C until  
148 analysed on the Flow Cytometer.

149 For characterization of transduced cell populations, samples were washed two times  
150 in FACS buffer, and surface staining was performed for 30 min at 4 °C. The following  
151 antibodies were used in FACS buffer: anti-CD11c (clone: B-Ly6, BD Biosciences), -CD19 (clone:  
152 HIB19, BioLegend), -CD16 (clone: 3G8, BioLegend and BD Biosciences), -HLA-DR (clone: G46-  
153 6, BioLegend), -CD123 (clone: 6H6, BioLegend), -CD14 (clone: M5E2, BioLegend), -CD3 $\epsilon$   
154 (clone: UCHT1, BioLegend), and -CD56 (NCAM16.2, BioLegend). After surface staining,  
155 samples were washed two times in FACS buffer, and cells were fixed and permeabilized for  
156 20 min at 4 °C using Cytofix/Cytoperm (BD Biosciences). Samples were washed two additional  
157 times in FACS buffer and stored at 4 °C until analysed on the flow cytometer. If applicable,  
158 intracellular staining for IFN- $\alpha$ 2 (clone: 7N4-1, BD Biosciences) was performed following the  
159 fixation step. Samples were washed two times in Perm/Wash buffer, and stained in  
160 Perm/Wash buffer for 30 min at 4 °C. Following intracellular staining, samples were washed  
161 two additional times in Perm/Wash buffer, and stored in FACS buffer at 4 °C until analysed  
162 on the flow cytometer.

163 **Characterization of murine MAIT and iNKT cells.** Following tetramer staining (above), surface  
164 staining was performed in FACS buffer for 30 min at 4 °C. The following antibodies were used:  
165 anti-CD69 (clone: H1.2F3), -B220 (clone: RA3-6B2), -F4/80 (clone: BM8), -CD44 (clone: IM7),  
166 and -TCR $\beta$  (clone: H57-597), and fixable live/dead vital dye. All antibodies purchased from  
167 BioLegend and vital dye was from Life Technologies. After surface staining, samples were  
168 washed two times in FACS buffer, and cells were fixed and permeabilized for 20 min at 4 °C  
169 using Cytofix/Cytoperm (BD Biosciences). Cells were subsequently washed two times in  
170 Perm/Wash buffer (BD Biosciences). Intracellular staining was performed for 30 min at 4 °C  
171 and anti-granzyme B (clone: GB11, BD Biosciences) was added in Perm/Wash buffer.

172 Following intracellular staining, samples were washed two additional times in Perm/Wash  
173 buffer, and stored in FACS buffer at 4 °C until analysed on the flow cytometer.

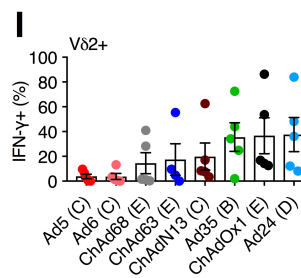
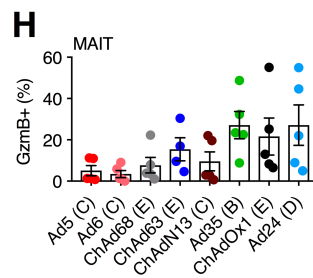
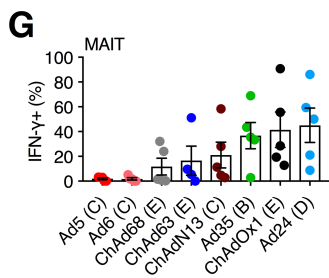
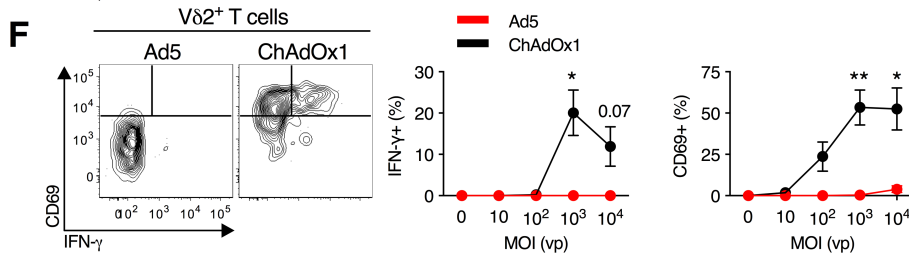
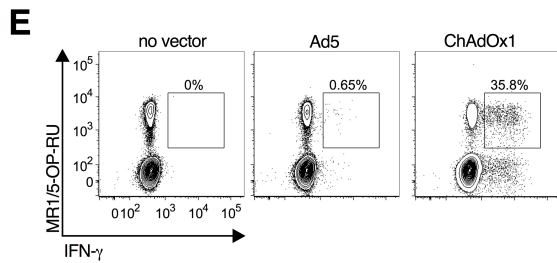
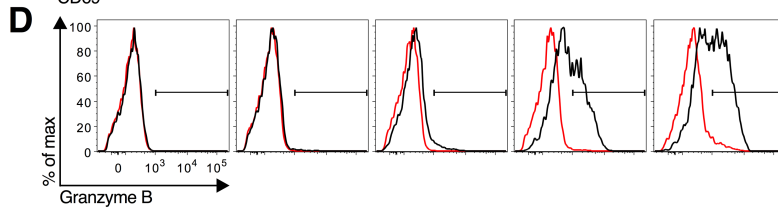
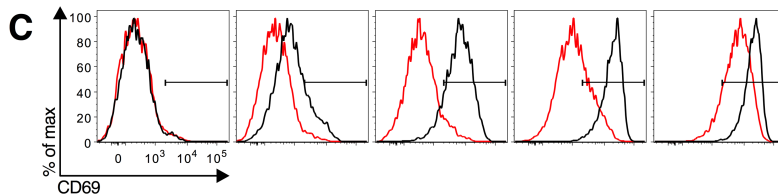
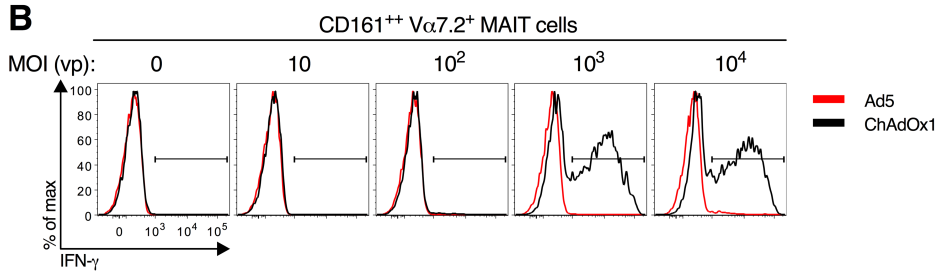
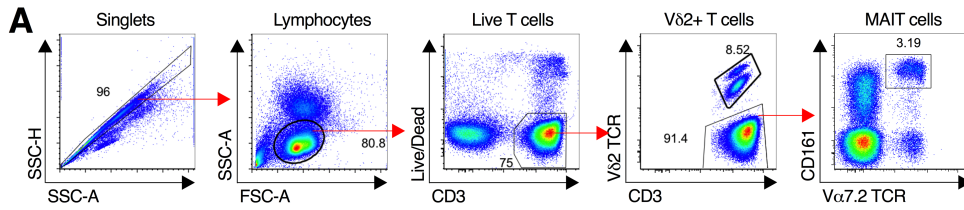
174 **Peptide stimulation and intracellular cytokine staining of mouse splenocytes.** Peptide re-  
175 stimulation of mouse splenocytes was performed as previously described(30). Briefly, 15-mer  
176 peptides of the HCV genotype 1b (overlapping by 11 amino acids) were used at a final  
177 concentration of 1 µg/ml to stimulate splenocytes for 5 h at 37 °C in 5% CO<sub>2</sub>. Brefeldin A (final  
178 concentration of 5 µg/ml; BioLegend) and anti-CD107a antibody (clone: 1D4B, BioLegend)  
179 were added at the time of peptide addition. Following stimulation, cells were washed one  
180 time in FACS buffer and surface staining was performed for 30 min at 4 °C. The following  
181 antibodies were used: anti-CD8a (clone: 53-6.7), -CD4 (clone: RM4-5), -CD44 (clone: IM7), -  
182 CD127 (clone: A7R34), and -KLRG1 (clone: 2F1), and Fixable Live/Dead vital dye. All antibodies  
183 purchased from BioLegend and vital dye was from Life Technologies. After surface staining,  
184 samples were washed two times in FACS buffer, and cells were fixed and permeabilized for  
185 20 min at 4 °C using Cytofix/Cytoperm (BD Biosciences). Cells were subsequently washed two  
186 times in Perm/Wash buffer (BD Bioscience). Intracellular staining was performed for 30 min  
187 at 4 °C and anti-IFN-γ (clone: XMG1.2, BioLegend) and anti-TNF-α (clone: MP6-XT22,  
188 BioLegend) were added in Perm/Wash buffer. Following intracellular staining, samples were  
189 washed two additional times in Perm/Wash buffer, and stored in FACS buffer at 4 °C until  
190 analysed on the flow cytometer.

191 **Data analysis and statistics.** All flow cytometry data was acquired on a BD Fortessa Flow  
192 Cytometer (BD Biosciences) and processed in FlowJo v. 9.9.6 (FlowJo, LLC). For analysis of the  
193 Human XL Cytokine Array, the developed film was scanned (Canon C-EXV), images were  
194 converted to greyscale, and pixel density was quantified using ImageJ (v. 1.51). Only  
195 membrane spots visible to the naked eye were considered to be positive. All data was  
196 analyzed in Prism v. 8.0.1 (GraphPad). For analysis of vaccinated human volunteers, a non-  
197 parametric paired Wilcoxon Rank Sum Test was used. For analysis of *in vitro* stimulations,  
198 unpaired Student T tests were used for comparison of two groups. A repeated-measures one-  
199 way ANOVA with a Dunnett correction for multiple comparisons was used, or a mixed-effects  
200 model with Dunnett correction for multiple comparisons was used if there were different  
201 numbers of data points in each group. For analysis of dose response curves, a test for linear  
202 trend was performed. For analysis of *in vivo* mouse data, a one-way ANOVA was performed



203 with a Dunnett correction for multiple comparisons. For all tests,  $P < 0.05$  was considered  
204 statistically significant, and  $P < 0.1$  was considered a trend with the exact P value reported.  
205

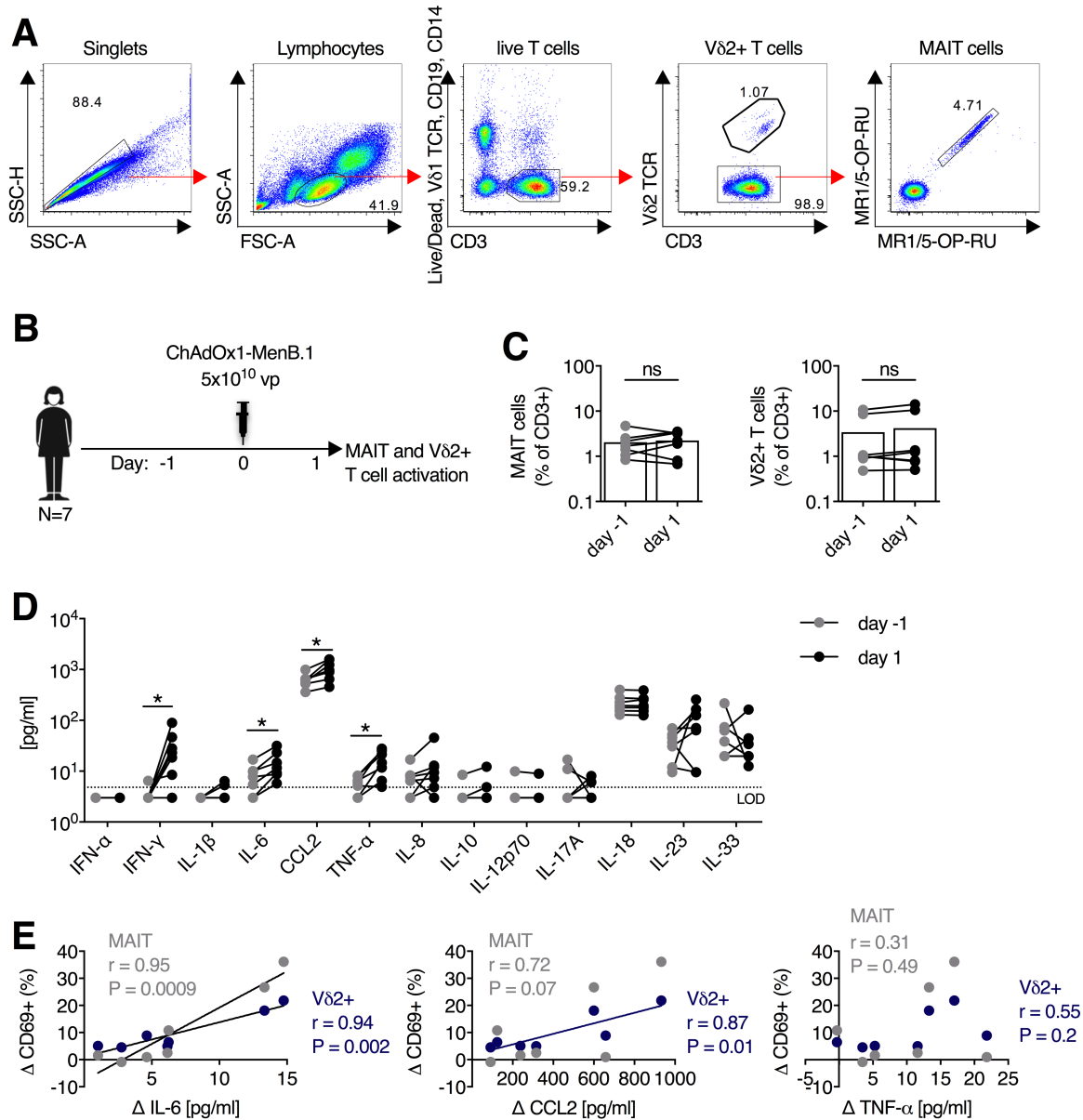
206 **Supplemental Figures and Legends**



208 **Figure S1. (A)** Gating scheme for the identification of MAIT cells (CD161<sup>++</sup>V $\alpha$ 7.2<sup>+</sup> T cells) and  
209 V $\delta$ 2<sup>+</sup> T cells in human PBMCs. **(B-D)** PBMCs were stimulated with Ad5 or ChAdOx1 at  
210 increasing MOIs (0 to 10<sup>4</sup> vp), and IFN- $\gamma$  **(B)**, CD69 **(C)**, and granzyme B (GzmB) **(D)** expression  
211 was measured on MAIT cells after 24 h. Representative flow cytometry plots are shown;  
212 relates to Fig 1a-c. **(E)** Fresh human PBMCs were stimulated for 24 h with Ad5 or ChAdOx1  
213 (MOI=10<sup>3</sup> vp), and IFN- $\gamma$  production by MAIT cells identified using MR1/5-OP-RU tetramers  
214 was assessed after 24 h. Data are representative of N=2 donors. **(F)** IFN- $\gamma$  and CD69 expression  
215 on V $\delta$ 2<sup>+</sup> T cells was measured after 24 h stimulation of PBMCs (N=3) with Ad5 or ChAdOx1 at  
216 the indicated MOI. Representative flow cytometry plots (MOI=10<sup>3</sup> vp) and group averages are  
217 shown. **(G-I)** Fresh human PBMCs (N=5) were stimulated with the indicated Ad-vector (species  
218 noted in parentheses), and IFN- $\gamma$  **(G)** or GzmB **(H)** production by MAIT, and IFN- $\gamma$  production  
219 by V $\delta$ 2<sup>+</sup> T cells **(I)** was measured after 24 h. These data are the individual donor data that  
220 relate to Figure 1. \*, <0.05; \*\*, P<0.01. Unpaired T test **(F)**. Symbols indicate individual donors,  
221 and mean  $\pm$  SEM are shown.

222

223



224

225 **Figure S2. (A)** Gating scheme for the identification of MAIT cells (MR1/5-OP-RU++ T cells) and

226 Vδ2+ T cells in PBMCs of healthy human volunteers immunized with ChAdOx1. **(B)** Healthy

227 human volunteers (N=7) were immunized with a 5x10<sup>10</sup> vp dose of ChAdOx1 expressing a *N.*

228 *meningitidis* group B antigen (MenB.1). **(C)** Frequencies of MAIT cells and Vδ2+ T cells in

229 peripheral blood one day pre- and one day post-immunization. **(D)** Concentration of plasma

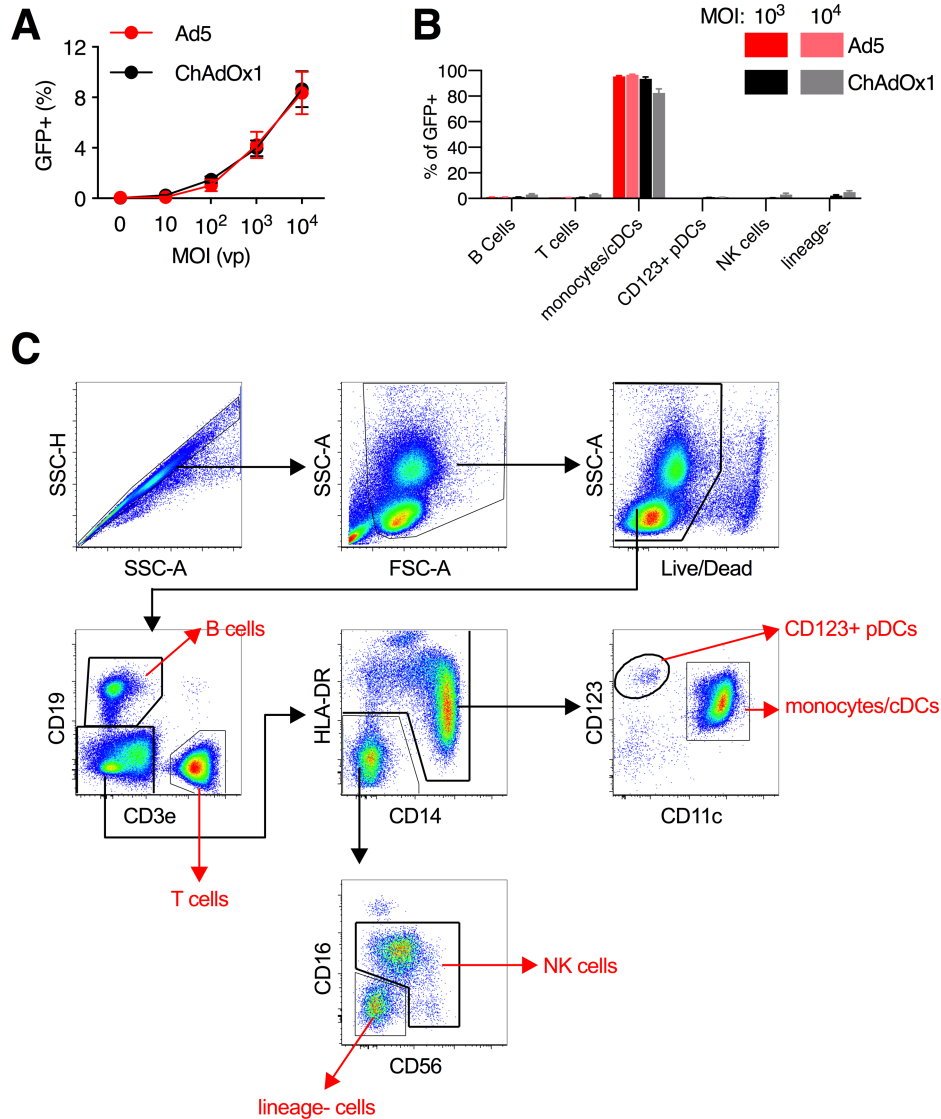
230 cytokine levels in healthy human volunteers (N=7) one day pre- and one day post-

231 immunization with 5x10<sup>10</sup> vp of ChAdOx1-MenB.1. **(E)** Pearson correlation of change in

232 cytokine level following vaccination and the change in expression of CD69 on MAIT cells and

233 Vδ2+ T cells. \*, P<0.05; Wilcoxon rank-sum test. Symbols indicate individual donors, and

234 group mean is shown.



235

236 **Figure S3. (A,B)** Fresh human PBMCs were stimulated for 24 h with either Ad5 or ChAdOx1

237 expressing GFP at the indicated MOI (in vp). **(A)** Fraction of all live PBMCs (N=9) that were

238 GFP+ after 24 h. **(B)** The fraction of GFP+ cells (N=3 donors) that were B cells (CD19+), T cells

239 (CD3+), Monocytes/cDCs (HLA-DR+ CD11c+ CD19- CD3-), CD123+ pDCs (CD123+ CD11c- HLA-

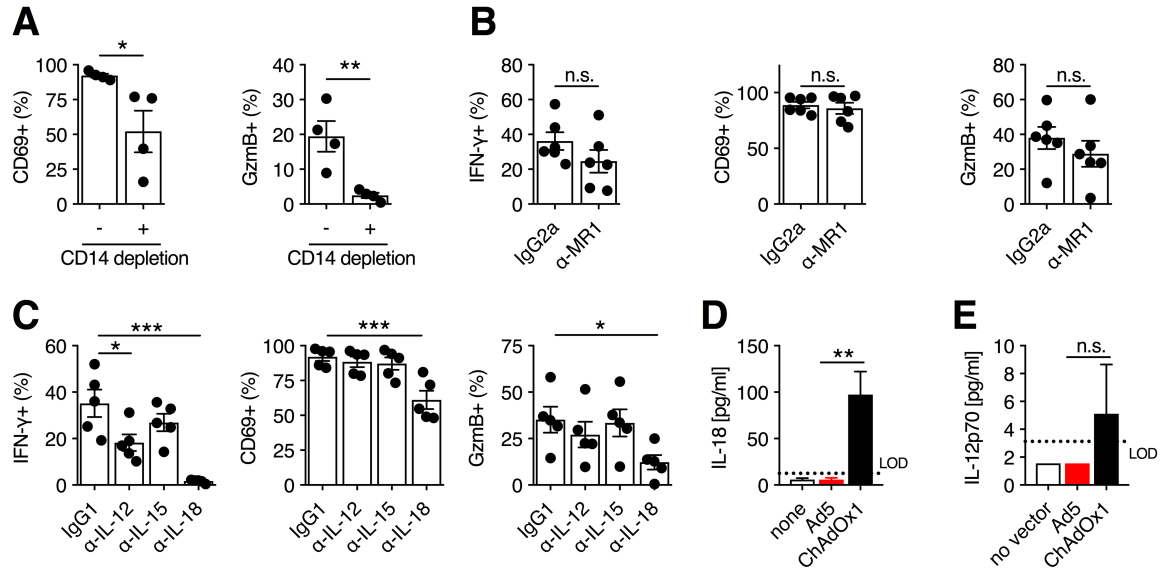
240 DR+ CD3- CD 19-), NK cells (CD56+ CD3-), or lineage- cells (HLA-DR- CD19- CD3- CD56-)

241 was enumerated. **(C)** Gating scheme for the identification of major immune cell subsets within

242 human PBMCs.

243

244

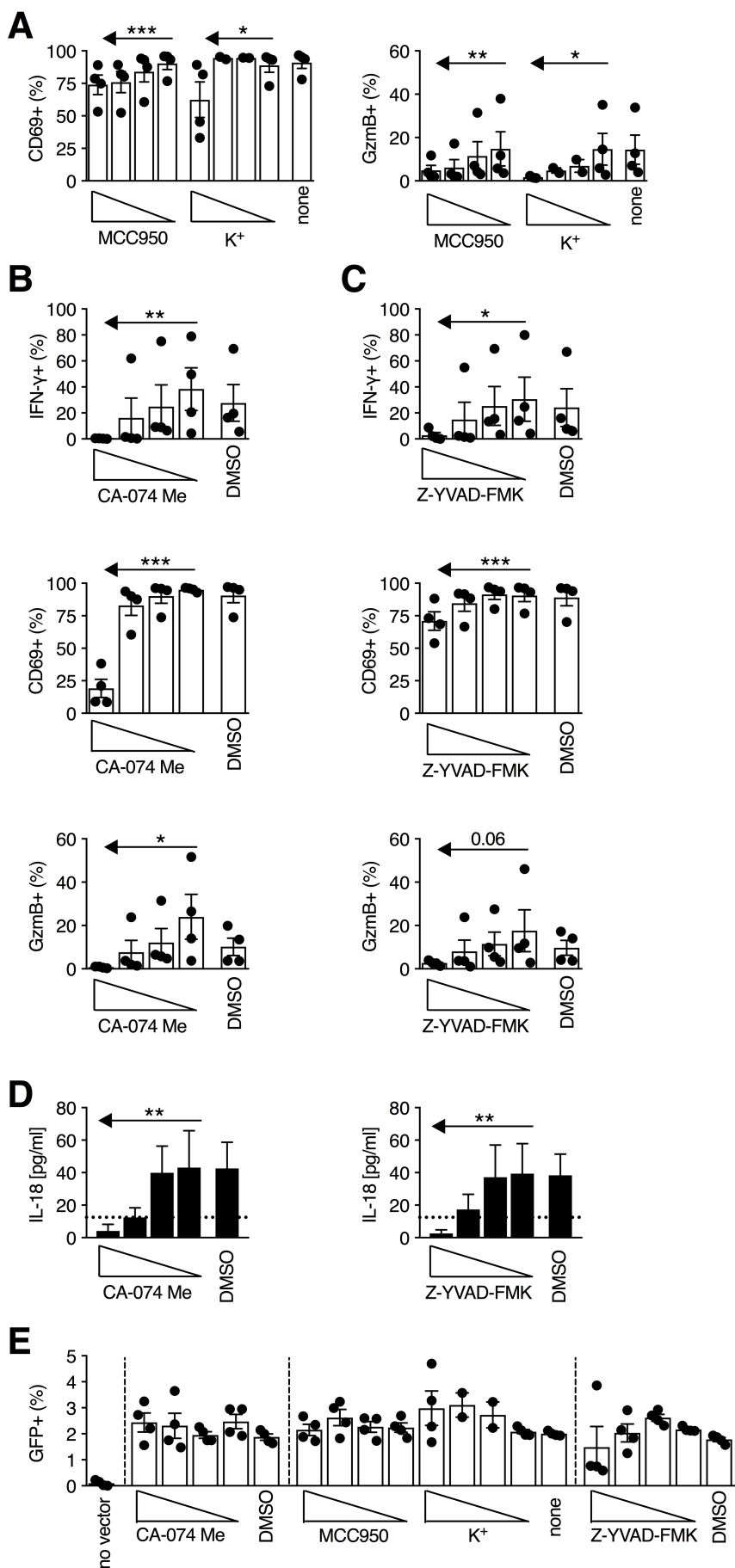


245

246 **Figure S4. (A)** PBMCs were depleted of CD14<sup>+</sup> monocytes or left untreated as a control (N=4),  
 247 and were stimulated with ChAdOx1 (MOI= 10<sup>3</sup> vp). CD69 and granzyme B (GzmB) expression  
 248 was measured on MAIT cells (CD161<sup>+</sup>+Vα7.2<sup>+</sup> T cells) after 24 h. **(B)** Fresh human PBMCs  
 249 were treated with anti-MR1 antibody (10 μg/ml, N=6) immediately prior to stimulation with  
 250 ChAdOx1 vectors (MOI=10<sup>3</sup> vp), and IFN-γ, CD69, and GzmB expression on MAIT cells was  
 251 measured after 24 h. **(C)** PBMCs (N=5) were stimulated with ChAdOx1 (MOI=10<sup>3</sup> vp), and anti-  
 252 IL-12, anti-IL-15, or anti-IL-18 antibodies (10 μg/ml) were added immediately prior to vector  
 253 addition. IFN-γ, CD69, and GzmB expression was measured on MAIT cells after 24 h.  
 254 Concentration of IL-18 **(D)** and IL-12p70 **(E)** in cell culture supernatants following 24 h  
 255 stimulation of fresh PBMCs with Ad5 or ChAdOx1 (MOI=10<sup>3</sup> vp). \*, P<0.05; \*\*, P<0.01; \*\*\*,  
 256 P<0.001. Unpaired T test **(A,B,D,E)** and repeated-measures one-way ANOVA with Dunnett  
 257 correction **(C)**. Symbols indicate individual donors, and mean ± SEM are shown.

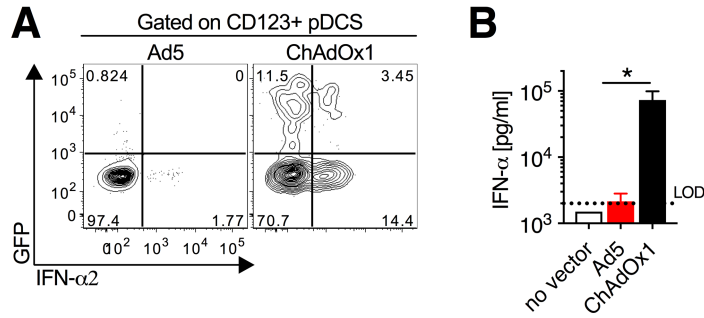
258

259





261 **Figure S5. (A)** The NLPR3 inhibitors (MCC950 [0.01-10  $\mu$ M]) and extracellular K<sup>+</sup> [5-30 mM])  
262 were added immediately prior to stimulation of PBMCs with ChAdOx1 (MOI=10<sup>3</sup> vp), and  
263 CD69 and granzyme B (GzmB) production by MAIT cells (CD161++V $\alpha$ 7.2+ T cells) was assessed  
264 after 24 h (N=4). Cathepsin B inhibitor (CA-074-Me [0.01-10  $\mu$ M]) **(B)** and Caspase 1 inhibitor  
265 (Z-YVAD-FMK [0.1-100  $\mu$ M]) **(C)** were added immediately prior to stimulation of PBMCs with  
266 ChAdOx1 (MOI=10<sup>3</sup> vp). After 24 h, IFN- $\gamma$ , CD69, and GzmB production by MAIT cells was  
267 assessed (N=4). **(D)** Concentration of IL-18 in cell culture supernatants of PBMCs treated with  
268 the indicated inhibitors 24 h after stimulation with ChAdOx1 MOI=10<sup>3</sup> vp; N=4). **(E)** Frequency  
269 of GFP+ PBMCs (N=4) at 24 h following transduction with ChAdOx1 expressing GFP (MOI=10<sup>3</sup>  
270 vp) in the presence of the indicated dose of CA-074 Me, MCC950, extracellular K<sup>+</sup> ions, or Z-  
271 YVAD-FMK. \*, P<0.05; \*\*, P<0.01; \*\*\*, P<0.001. Repeated-measures one-way ANOVA with  
272 test for linear trend. Symbols indicate individual donors, and mean  $\pm$  SEM are shown.  
273  
274

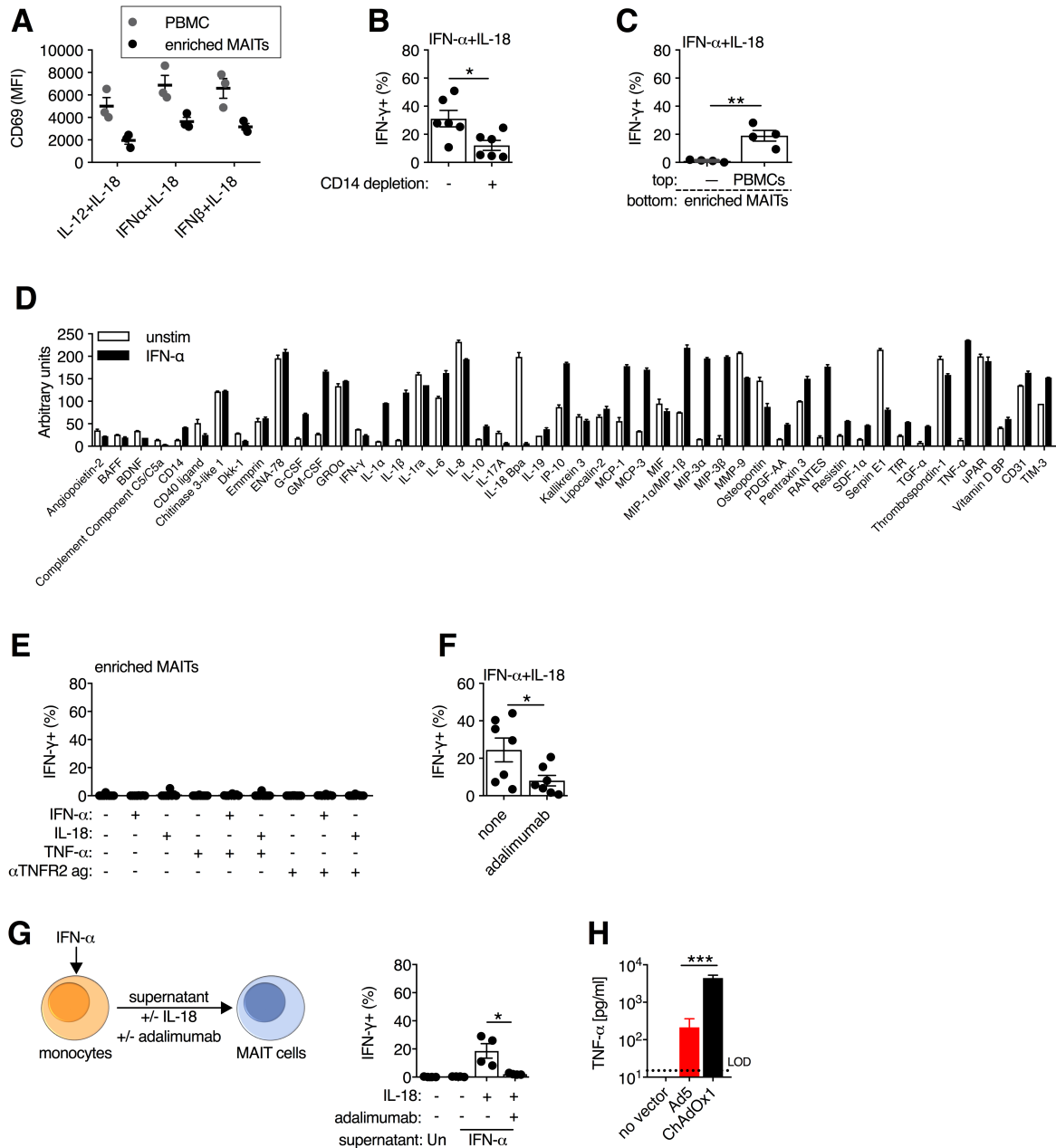


275

276 **Figure S6. (A)** Expression of IFN- $\alpha$ 2 on CD123+ pDCs (HLA-DR+ CD11c- CD14- CD16- CD19-  
277 CD3-) 24 h after stimulation with Ad5 or ChAdOx1 expressing GFP (MOI=10<sup>3</sup> vp). Data are  
278 representative of N=4 donors. **(B)** Concentration of IFN- $\alpha$  in cell culture supernatants  
279 following 24 h stimulation of fresh PBMCs with Ad5 or ChAdOx1 (MOI=10<sup>3</sup> vp). \*, P<0.05.  
280 Unpaired T test **(B)**. Mean  $\pm$  SEM are shown.

281

282



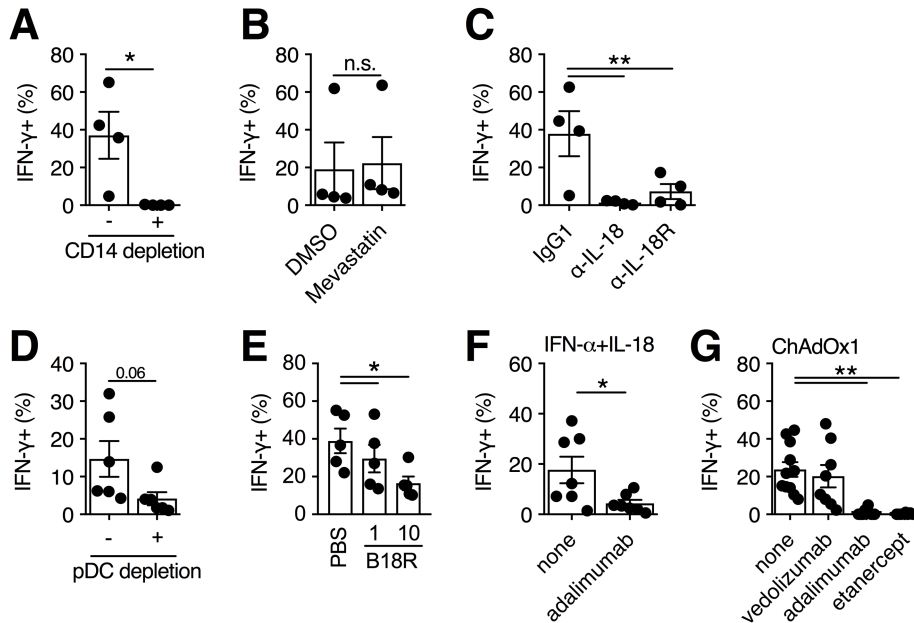
283

284 **Figure S7. (A)** Unfractionated PBMCs or enriched MAIT cells (positive selection by CD8  
 285 MicroBeads) were stimulated for 24 h with the indicated cytokines (50 ng/ml), and CD69  
 286 expression was measured on MAIT cells after 24 h. **(B)** Unfractionated PBMCs or CD14+  
 287 monocyte-depleted PBMCs were stimulated with IFN- $\alpha$  + IL-18 (50 ng/ml), and IFN- $\gamma$   
 288 production by enriched MAIT cells was measured after 24 h (N=6). **(C)** Using a 0.3  $\mu$ m  
 289 transwell system, enriched MAIT cells were placed in the bottom chamber and the top  
 290 chamber was loaded with either autologous PBMCs or left cell-free (N=4). IFN- $\gamma$  production  
 291 by MAIT cells was assessed at 24 h following stimulation with IFN- $\alpha$  + IL-18 (50 ng/ml). **(D)**  
 292 CD14-purified monocytes (N=1, in duplicate) were stimulated with IFN- $\alpha$  (50 ng/ml) or left

293 untreated. After 24 h, supernatants were collected and used fresh for immunoblotting.  
294 Relative protein concentration was calculated by quantifying pixel density. **(E)** CD8-  
295 MicroBead enriched MAIT cells (N=10) were stimulated with single or double combinations  
296 of IFN- $\alpha$ , IL-18, TNF- $\alpha$ , or anti-TNFR2 agonist antibody (cytokine at 50 ng/ml and agonist  
297 antibody at 2.5  $\mu$ g/ml). IFN- $\gamma$  production by MAIT cells was measured after 24 h. **(F)** PBMCs  
298 (N=7) were stimulated with IFN- $\alpha$  + IL-18 (50 ng/ml), and adalimumab (anti-TNF- $\alpha$  antibody;  
299 10  $\mu$ g/ml) was added immediately prior cytokine addition. IFN- $\gamma$  production by MAIT cells was  
300 measured after 24 h. **(G)** Purified monocytes (N=4) were stimulated with IFN- $\alpha$  (50 ng/ml), or  
301 left untreated, and after 24 h supernatants were transferred to autologous enriched MAIT  
302 cells  $\pm$  IL-18 (50 ng/ml) and  $\pm$  adalimumab (anti-TNF- $\alpha$  antibody; 10  $\mu$ g/ml). IFN- $\gamma$  production  
303 by MAIT cells was measured at 24 h. **(H)** Concentration of TNF- $\alpha$  in cell culture supernatants  
304 of PBMCs 24 h after stimulation with Ad5 or ChAdOx1 (MOI=10<sup>3</sup> vp; N=7). \*, P<0.05; \*\*,  
305 P<0.01; \*\*\*, P<0.001. Unpaired T test. Symbols indicate individual donors, and mean  $\pm$  SEM  
306 are shown.

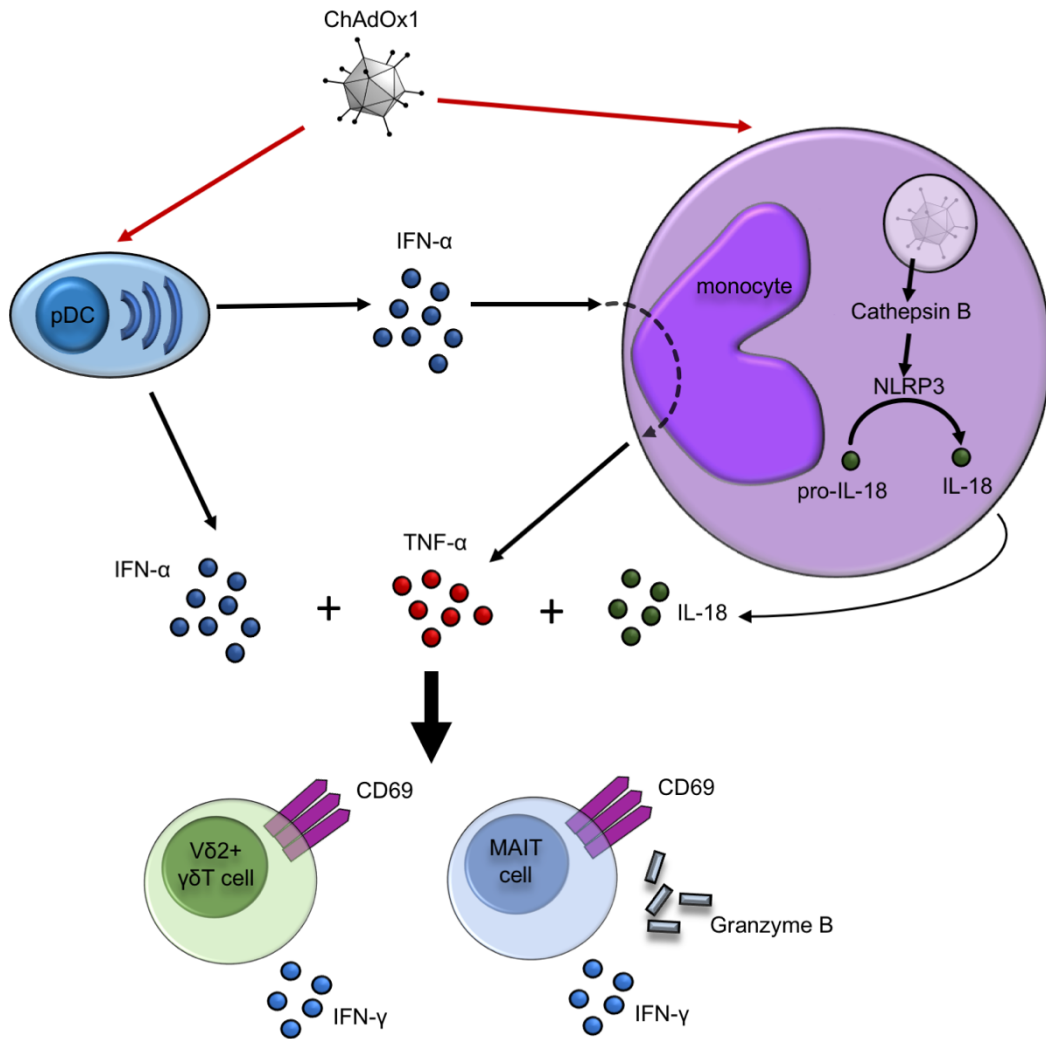
307

308



309

310 **Figure S8. (A)** Fresh human PBMCs were depleted of CD14+ monocytes or left untreated as a  
 311 control (N=4), and were stimulated with ChAdOx1 (MOI=10<sup>3</sup> vp). IFN- $\gamma$  production by V $\delta$ 2+ T  
 312 cells was measured after 24 h. **(B,C)** Fresh human PBMCs were treated with mevastatin (5  
 313  $\mu$ M; N=4) **(B)**, or either anti-IL-18 or anti-IL-18R antibodies (10  $\mu$ g/ml; N=4) **(C)** immediately  
 314 prior to addition of ChAdOx1 (MOI=10<sup>3</sup> vp). IFN- $\gamma$  production by V $\delta$ 2+ T cells was measured  
 315 after 24 h. **(D)** PBMCs were depleted of CD123+ pDCs or left untreated as a control (N=4), and  
 316 IFN- $\gamma$  expression was measured on V $\delta$ 2+ T cells after 24 h stimulation with ChAdOx1 (MOI=10<sup>3</sup>  
 317 vp). **(E)** PBMCs (N=5) were stimulated with ChAdOx1 (MOI=10<sup>3</sup> vp), and B18R (1 or 10  $\mu$ g/ml)  
 318 was added immediately prior to vector addition. IFN- $\gamma$  production by V $\delta$ 2+ T cells was  
 319 measured after 24 h. **(F)** PBMCs (N=7) were stimulated with IFN- $\alpha$  + IL-18 (50 ng/ml), and  
 320 adalimumab (anti-TNF- $\alpha$  antibody; 10  $\mu$ g/ml) was added immediately prior to cytokine  
 321 addition. IFN- $\gamma$  production by V $\delta$ 2+ T cells was measured after 24 h. **(G)** PBMCs were  
 322 stimulated with ChAdOx1 (MOI=10<sup>3</sup> vp), and vedolizumab (anti- $\alpha$ 4 $\beta$ 7 integrin antibody, N=8),  
 323 adalimumab (anti-TNF- $\alpha$  antibody, N=11), or etanercept (TNFR2-Fc fusion protein, N=8) (10  
 324  $\mu$ g/ml) was added immediately prior to vector addition. IFN- $\gamma$  production by V $\delta$ 2+ T cells was  
 325 measured after 24 h. \*, P<0.05; \*\*, P<0.01. Unpaired T test. **(A,B,D,F)** and repeated-measures  
 326 one-way ANOVA with Dunnett Correction **(C,E,G)**. Symbols indicate individual donors, and  
 327 mean  $\pm$  SEM are shown.

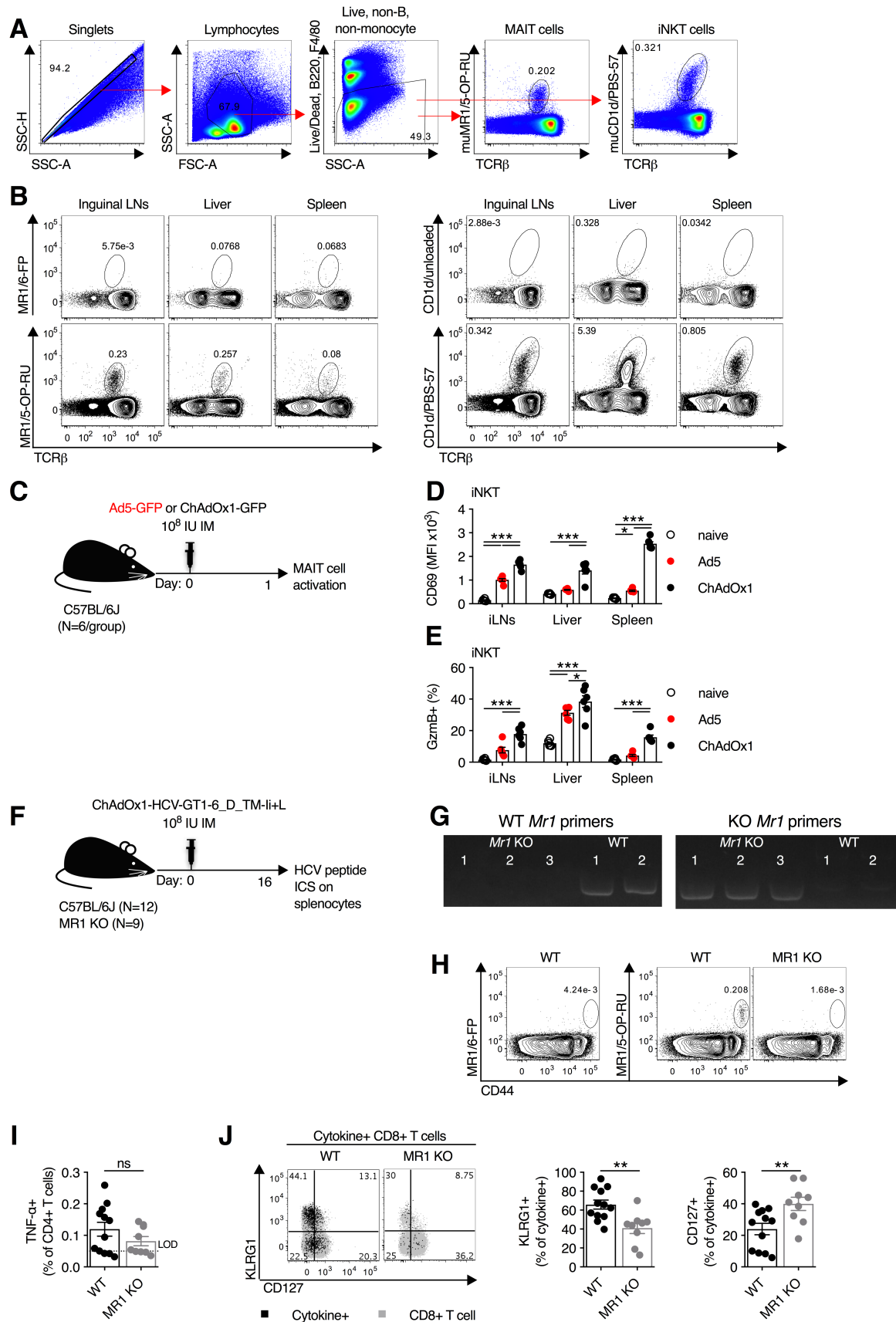


328

329 **Figure S9.** Model for how ChAdOx1 (and other stimulatory Ad vectors) activates MAIT cells  
330 and Vδ2+ T cells. Activation involves two pathways: (1) ChAdOx1 transduces monocytes and  
331 induces IL-18 production by activating the NLRP3 inflammasome, and (2) ChAdOx1 transduces  
332 pDCs and triggers the production of IFN-α, which in turn drives TNF-α production by  
333 monocytes. The combination of IL-18, IFN-α, and TNF-α act on MAIT and Vδ2+ T cells to  
334 induce expression of IFN-γ, Granzyme B, and CD69.

335

336



337

338 **Figure S10. (A)** Gating scheme for the identification of MAIT cells and iNKT cells in mice using  
 339 MR1 and CD1d tetramers. **(B)** Representative flow cytometry plots of the frequency of MAIT

340 cells and iNKT cells in the inguinal LNs, liver, and spleen of C57BL/6 mice. **(C-E)** C57BL/6J mice  
341 (N=6 per group) were immunized intramuscularly with  $10^8$  IU of Ad5 or ChAdOx1 expressing  
342 GFP **(C)**, and one day post-immunization expression of CD69 **(D)** and granzyme B (GzmB) **(E)**  
343 was measured on iNKT cells (CD1d/PBS-57+ T cells) isolated from inguinal LNs, liver, and  
344 spleen. Data are representative of two independent experiments. **(F-J)** C57BL/6J (N=12) or  
345 MR1 KO (N=9) mice were immunized intramuscularly with  $10^8$  IU of ChAdOx1 expressing HCV-  
346 GT1-6\_D\_TM-li+L transgene, and on day 16 post-immunization splenocytes were collected  
347 **(F)**. **(G,H)** Genotyping of wild-type C57BL/6 and MR1 KO mice by PCR for the *Mr1* gene **(G)**  
348 and confirmation of the absence of MAIT cells in the inguinal LNs by flow cytometry **(H)**. **(I)**  
349 Group averages for TNF- $\alpha$  production by CD4 T cells following 5 h restimulation with an  
350 overlapping peptide pool of the HCV genotype 1b proteome. **(J)** Representative flow  
351 cytometry plots and group averages of KLRG1 and CD127 expression on cytokine-producing  
352 CD8 T cells following peptide restimulation. \*, P<0.05; \*\*, P<0.01; \*\*\*, P<0.001. One-way  
353 ANOVA with Sidak correction for multiple comparisons **(D,E)** and unpaired T test **(I,J)**. Symbols  
354 indicate individual animals, and mean  $\pm$  SEM are shown.  
355